T/C

COO-3130TB-254

PROGRESS REPORT OF A RESEARCH PROGRAM IN EXPERIMENTAL HIGH ENERGY PHYSICS

Progress Report
for Period January 1, 1980 - December 31, 1980

Anatole M. Shapiro and Mildred Widgoff

Brown University

Providence, Rhode Island

October 1, 1980

PREPARED FOR THE U.S. DEPARTMENT OF ENERGY UNDER CONTRACT DE-AC02-76ER03130.A006
(TASK B-EXPERIMENTAL)

DISCLAIMER

NOTICE

ABSTRACT

An experimental program to study the interactions of hadrons and photons is being carried out using hybrid systems which include bubble chambers as visible targets as well as counter spectrometers. Experiments are being performed at the accelerators of the laboratories at Batavia, Stanford, and Geneva, Switzerland.

The bubble chamber - hybrid system group is engaged in several experiments at Fermilab. Extensive analysis of the interactions of 147 GeV/c π^+, K^+, and p in hydrogen is in progress; the results of our earlier experiment on π^-p interactions at the same momentum, in the same experimental set-up, are available for comparison, thus extending the range of incident-channel quantum numbers studied with a minimum of systematic error. This year there has been particular emphasis on associated production in interactions of the form $ab \rightarrow cX$, on ρ^o production, and on multi-particle correlations. Comparison of hadron production by hadrons with hadron production by leptons is being extended to all our incident particles, for a variety of kinematic variables. Two experiments with an improved hybrid system are now scheduled for data-taking at Fermilab in early 1981, to study $\pi^\pm$, K^+ and $p^\pm$ interactions in hydrogen, and in aluminum, silver, and gold foils, at beam momenta of 200 and 400 GeV/c. A similar study at 250 GeV/c, using the large European Hybrid System at CERN, will begin during 1981. During the spring and summer of 1980, data-taking was begun on two experiments investigating photoproduction of charm and vector mesons, in a polarized monoenergetic backscattered laser beam of 20 GeV/c using the SLAC Hybrid Facility.

Progress Report of a Research Program in Experimental High Energy Physics

The Department of Physics of Brown University presents herein a report of the progress made in the experimental program during the present contract period (1 January 1980 - 31 December 1980). This work has been supported by the U.S. Department of Energy under Contract DE-AC02-76ER0-3130.A006 (Task B-Experimental).

This report on the bubble chamber-proportional hybrid system program is divided as follows:

I. Data Analysis in Progress

II. Experimental Runs in Progress and in Preparation

III. Associated Matters

IV. Scientific Personnel

V. Papers Published During the Preceding Year and Papers in Press

I. Data Analysis in Progress.

(a) Studies of $\pi^+ p$, $K^+ p$, and pp Interactions at 147 GeV/c (FNAL Experiment 299) and of $\pi^- p$ Interactions at 147 GeV/c (FNAL Experiment 154) using the Proportional Wire Chamber-Bubble Chamber Hybrid System at Fermilab.

These two experiments are complementary studies of the characteristics of high energy strong interactions as a function of the properties of the four incident projectile particles.

Experiment 154 is essentially completed, with a few remaining papers in the process of being prepared and published. Two papers appeared during the past year in Physical Review D (see Section V, References 320 and 324). However, the data from E-154 are being used more and more in comparisons with the data from E-299.

The data of E-299 were obtained from two exposures of the Fermilab Proportional Wire Chamber - 30 inch Bubble Chamber Hybrid System (PHS) in tagged beams of positive particles of 147 GeV/c momentum. The portion of the hybrid system upstream of the bubble chamber provides for the identification of incoming particles by Cerenkov counters, and for the precise determination of their direction and momentum by proportional wire counters. Proportional wire chambers in the downstream portion of the hybrid system provide precise measurement of the momentum and direction of fast forward-going charged particles emerging through the fringing field of the bubble-chamber magnet. The bubble chamber itself serves as the target and provides complete solid angle sensitivity for all charged particles produced in any interaction in the chamber, and considerable detection efficiency for associated V^o's and γ's as well. The linking of the electronic data with the tracks in the bubble

chamber allows us to use the upstream Cerenkov signal to identify each interacting beam particle, so that we obtain data simultaneously for all the kinds of particles present in the beam, and can make comparisons with a minimum of systematic errors.

The first 158,000 frames were obtained in a beam of positive particles divided approximately equally between π^+ mesons and protons, with only a small percentage of K^+. An enrichment of the K^+ component of the beam to about 10 percent was achieved for the second positive beam run, consisting of 240,000 pictures, and this second run was further enhanced by the use of a prototype of the forward gamma detector which has been built for Experiments E-565 and E-570. This prototype was full scale except in area perpendicular to the beam, which was 30 cm x 30 cm rather than the final 75 cm x 75 cm. These prototype data allow us to analyze the forward-going electromagnetic radiation produced in the observed interactions, within the small solid angle subtended.

All of the film has been scanned, predigitized, and precision measured, and final remeasurements are being made on the difficult events.

Results obtained thus far in this experiment, together with some comparisons with our $\pi^- p$ experiment, have been presented in published papers (see Section V, References 321 and 322), in contributed papers (References 327-335), and in papers in press (References 336-338). The reports on E-299 data represent preliminary analyses of the available data and work on all areas is continuing. Some of this work is described briefly on the following pages.

(i) Average Charged-Particle Multiplicities in Hadron Interactions at 147 GeV/c (Experiments E-299 and E-154).

We have extended our earlier study of inclusive $\pi^- p$ interactions at 147 GeV/c (E-154)[1] to $\pi^+ p$, $K^+ p$ and pp inclusive interactions at the same momentum (E-299). We are now able to compare a number of interactions of the type

$$a + b \rightarrow c + X, \qquad (1)$$

all measured with the same equipment. Specifically, we have now investigated the average multiplicity $\langle n_X \rangle$ of the system X produced in the following reactions:

$$\pi^+ p \rightarrow \pi^+_{fast} X \qquad (2)$$

$$\pi^+ p \rightarrow p_{slow} X \qquad (3)$$

$$K^+ p \rightarrow K^+_{fast} X \qquad (4)$$

$$K^+ p \rightarrow p_{slow} X \qquad (5)$$

$$pp \rightarrow p_{fast} X \qquad (6)$$

$$pp \rightarrow p_{slow} X \qquad (7)$$

as well as

$$\pi^- p \rightarrow \pi^-_{fast} X \qquad (8)$$

$$\pi^- p \rightarrow p_{slow} X. \qquad (9)$$

In all these interactions, the fast particle is required to have Feynman $x \geqslant 0.5$, and the slow proton is identified by ionization in the bubble chamber, this identification being possible for momenta less than 1.4 GeV/c. Fast-particle identification was not possible in the spectrometer of E-154 and E-299;

the assumption was made in each case that the fastest particle having the same charge as the beam particle carried all the same quantum numbers as the beam particle.

In addition to reactions (2) - (9), we have investigated the interactions

$$\pi^+ p \to \Lambda^o X, \qquad (10)$$

$$pp \to \Lambda^o X, \qquad (11)$$

and

$$\pi^- p \to \Lambda^o X, \qquad (12)$$

with no explicit momentum restriction on the Λ^o, but requiring a good Λ^o fit in the backward hemisphere. In all these interactions, the multiplicity $\langle n_X \rangle$ has been determined as a function of M_X^2, the square of the mass of the system X, and t, the momentum transfer from a to c.

For inelastic interactions of the form

$$a + b \to X, \qquad (13)$$

a number of models of multiparticle production (e.g. References 2-7) have predicted various functional forms of the dependence of $\langle n_X \rangle$ on s, the square of the total center-of-mass energy. While it is clear that inelastic pp data, spanning a region in s ranging from 10 to 20,000 GeV^2, requires more complicated functions, over limited regions of s the variation of $\langle n_X \rangle$ is very well fitted by functions of the form

$$\langle n_X \rangle = A + B \ln s. \qquad (14)$$

The same is true for inelastic reactions of other particles (Ref. 1, and sources quoted therein). Similarly, for inclusive reactions such as (2) - (12), where M_X is the total CM energy of the system X, functions of the form

$$\langle n_X \rangle = A + B \ln M_X^2 \qquad (15)$$

may be expected to fit the data, over the range in CM energy we are concerned with. In fact, in our data at 147 GeV/c, where we cover the region $20 \leq M_X^2 < 140\ (GeV/c^2)^2$, the data are well fitted by the functional forms which fit the whole pp inelastic range, as well as by functions of the form given in (15).

As examples of the results, we show in Figures 1 and 2 $\langle n_X \rangle$ as a function of M_X^2 for various regions in $|t|$, for reactions (2) and (7) respectively. We have similar data for all the reactions (2) - (9); too few Λ^o's have been found to justify breaking the data up into regions in t. The solid lines in the figures are fitted functions of the form given in (15). The slopes of these lines showed no significant dependence on t for any of the reactions, and the data for all $|t| < 2.0\ (GeV/c)^2$, for reactions (2), (4), (6), (8), and reactions (3), (5), (7), (9), are shown in Figures 3 and 4. The lines in these figures are also fitted functions of the form shown in (15). Since the parameters A of these functions are the calculated multiplicity values for $M_X^2 = 1$, rather far from the region covered by the data, and hence subject to considerable uncertainty, we have in fact used the function

$$\langle n_X \rangle = A' + B' \ln (M_X^2/53),$$

normalized so the values A' are the average fitted multiplicities at $M_X^2 = 53\ (GeV/c^2)^2$. The parameters A' and B' for reactions (2)-(12), for all $|t| < 2.0 (GeV/c^2)^2$, are shown in Table I.

Several points of interest emerge from these results:

(1) π^+ and π^- are seen to be in agreement with each other.

(2) As expected, $pp \rightarrow p_{fast}X$ is in agreement with $pp \rightarrow p_{slow}X$, within 2.5 standard deviations at worst.

(3) The values of the slope B' are consistent with the average 1.49±0.08, and this is in agreement with values obtained for other interactions, both inclusive and total. (See Table VIII in Ref. 1.)

The data thus appear to be consistent with a linear dependence on M_X^2, and even with a constant slope, for all hadron-hadron interactions. Moreover, weak and electromagnetic processes show similar results.[10]

(4). There remain significant differences in the values of A'.

We have analyzed these results in terms of a simple model[1] which is represented by the diagrams in Fig. 5. Fig. 5a represents total inelastic reactions, ab → X, and in the model the total multiplicity is considered to be the sum of a multiplicity contribution associated with particle a, a multiplicity associated with particle b, and a central core multiplicity. Such a diagram is consistent with some quark pictures, e.g. Ref. 6, which postulate a universal core multiplicity in hadron interactions, equal to n_o = B ln s, the differences among interactions being attributed to target and beam fragmentation. The second diagram is the analogous one for inclusive reactions, where E_{ac} is an exchanged entity appropriate to the ac vertex, and we consider X to be produced in the interaction of E_{ac} with b. The total multiplicity of the system X is then again a sum of "target" and "beam" multiplicities, plus a central core, n_o = B ln(M_X^2). The terms entering into the multiplicity are shown in Table II specifically for the individual interactions.

We take n_o = B ln (M_X^2/53) to be constant, and hence can, by taking differences between pairs of measured values of $\langle n_X \rangle$, find relative multiplicities associated with specific beam and target particles. For instance, the difference between the measured $\langle n_X \rangle$ values for the first and second reac-

tions gives a value for $n_{E_{\pi\pi}} - n_{E_{KK}}$. The difference between the fourth and fifth gives $n_{\pi^\pm} - n_{K^+}$. Some specific differences, all obtained from the data of our hybrid spectrometer measurements, are tabulated in Table III.

$n_{E_{KK}}$ is seen to be very similar to $n_{E_{\pi\pi}}$, and both are quite different from $n_{E_{pp}}$. Qualitatively one might expect a difference, because, while a Pomeron can be the exchange particle in all three interactions, a pion can be exchanged at the pp vertex, not at the $\pi\pi$ or KK vertices. $n_{E_{pp}}$ and $n_{E_{p\Lambda^o}}$ are found to be equal.

The difference between n_π and n_p is consistent, at least qualitatively, with quark model predictions of Capella et al.[8]; and a difference between n_π and n_K has been predicted by Gotsman et al.[9] on the basis of a mass difference between strange and non-strange quarks.

Mildred Widgoff presented a paper on this analysis at the Washington meeting of the American Physical Society this April (Reference 332). Further analysis is in progress, especially to check for the dependence on Feynman x, and to attempt a more quantitative comparison with quark models.

REFERENCES

1. D. Brick et al., Phys. Rev. D19, 743 (1979).

2. W.R. Frazer et al., Rev. Mod. Phys. 44, 284 (1972).

3. E.L. Feinberg, Phys. Rep. 5C, 240 (1972).

4. M. Garetto et al., Nuovo Cimento 38, 38 (1977).

5. D.M. Tow, Phys. Rev. D7, 3535 (1973).

6. S.J. Brodsky and J.F. Gunion, Phys. Rev. Lett. 37, 402 (1976).

7. A. Casher, J. Kogut and L. Susskind, Phys. Rev. Lett. 31, 792 (1978).

8. A. Capella et al., Preprint LPTPE79/23 (Orsay).

9. E. Gotsman et al., Phys. Letters 74B, 252 (1978).

10. J.W. Chapman et al., Phys. Rev. Lett. 36, 124 (1976), and references cited therein.

TABLE I: Fits to the Function $A' + B' \ln(M_X^2/53)$

Reaction	A'	B'	χ^2/NDF
$\pi^+ p \to \pi_f^+ X$	4.45±0.07	1.55±0.13	1.7
$\pi^- p \to \pi_f^- X$	4.35±0.08	1.65±0.15	1.8
$K^+ p \to K_f^+ X$	4.49±0.20	1.40±0.40	1.6
$pp \to p_f X$	4.82±0.07	1.00±0.12	1.3
$\pi^+ p \to p_s X$	5.24±0.06	1.30±0.11	2.8
$\pi^- p \to p_s X$	5.28±0.08	1.63±0.14	0.5
$K^+ p \to p_s X$	4.81±0.14	1.40±0.26	1.6
$pp \to p_s X$	4.85±0.06	1.30±0.12	1.6
$\pi^+ p \to \Lambda^o X$	5.89±0.38	1.41±0.40	1.3
$\pi^- p \to \Lambda^o X$	4.97±0.28	1.82±0.45	3.0
$pp \to \Lambda^o X$	4.83±0.30	1.95±0.44	0.1

TABLE II: Multiplicities Interpreted in Terms of the Model Illustrated in Fig. 5b, for Various Reactions

	$\langle n_X \rangle$ =
$\pi^{\pm}p \rightarrow \pi_f^{\pm}X$	$n_{E_{\pi\pi}} + n_o + n_p$
$K^{+}p \rightarrow K_f^{+}X$	$n_{E_{KK}} + n_o + n_p$
$pp \rightarrow p_fX$	$n_{E_{pp}} + n_o + n_p$
$\pi^{\pm}p \rightarrow p_sX$	$n_{E_{pp}} + n_o + n_{\pi^{\pm}}$
$K^{+}p \rightarrow p_sX$	$n_{E_{pp}} + n_o + n_{K^{+}}$
$pp \rightarrow p_sX$	$n_{E_{pp}} + n_o + n_p$
$\pi^{\pm}p \rightarrow \Lambda^{o}X$	$n_{E_{p\Lambda^o}} + n_o + n_{\pi^{\pm}}$
$pp \rightarrow \Lambda^{o}X$	$n_{E_{p\Lambda^o}} + n_o + n_p$

Table III: Relative Multiplicities Associated With Specific Particles

$n_{E_{KK}} - n_{E_{\pi\pi}}$	=	$A'(K^+p \to K_f^+X)$	−	$A'(\pi^\pm p \to \pi_f^\pm X)$	=	0.08 ± 0.15
$n_{e_{pp}} - n_{E_{\pi\pi}}$	=	$A'(pp \to pX)$	−	$A'(\pi^\pm p \to \pi_f^\pm X)$	=	0.43 ± 0.05
$n_{e_{pp}} - n_{E_{KK}}$	=	$A'(pp \to pX)$	−	$A'(K^+p \to K_f^+X)$	=	0.35 ± 0.15
$n_{\pi^\pm} - n_K$	=	$A'(\pi^\pm p \to p_s X)$	−	$A'(K^+p \to p_s X)$	=	0.45 ± 0.11
$n_{\pi^\pm} - n_p$	=	$A'(\pi^\pm p \to p_s X)$	−	$A'(pp \to pX)$	=	0.48 ± 0.10
	=	$A'(\pi^\pm p \to \Lambda^o X)$	−	$A'(pp \to \Lambda^o X)$		
$n_{K^+} - n_p$	=	$A'(K^+p \to p_s X)$	−	$A'(pp \to pX)$	=	-0.03 ± 0.11
$n_{E_{pp}} - n_{E_{p\Lambda}}$	=	$A'(\pi^\pm p \to p_s X)$	−	$A'(\pi^\pm p \to \Lambda^o X)$	=	-0.11 ± 0.40
	=	$A'(pp \to p_s X)$	−	$A'(pp \to \Lambda^o X)$		

$$\pi^+ + p \rightarrow \pi^+_{fast} + X$$

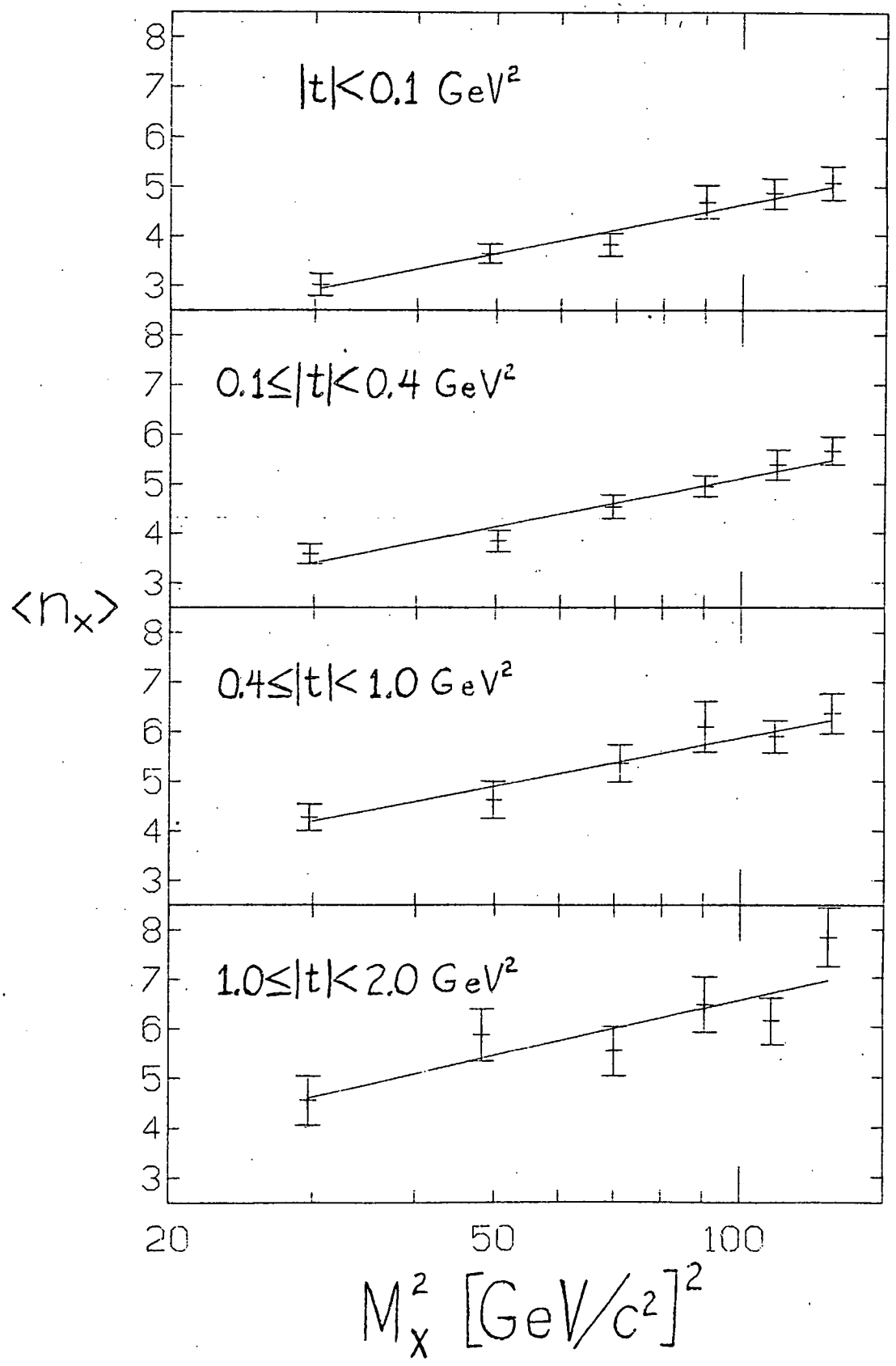

Fig. 1 (Ia) i)

$p + p \rightarrow p_{slow} + X$

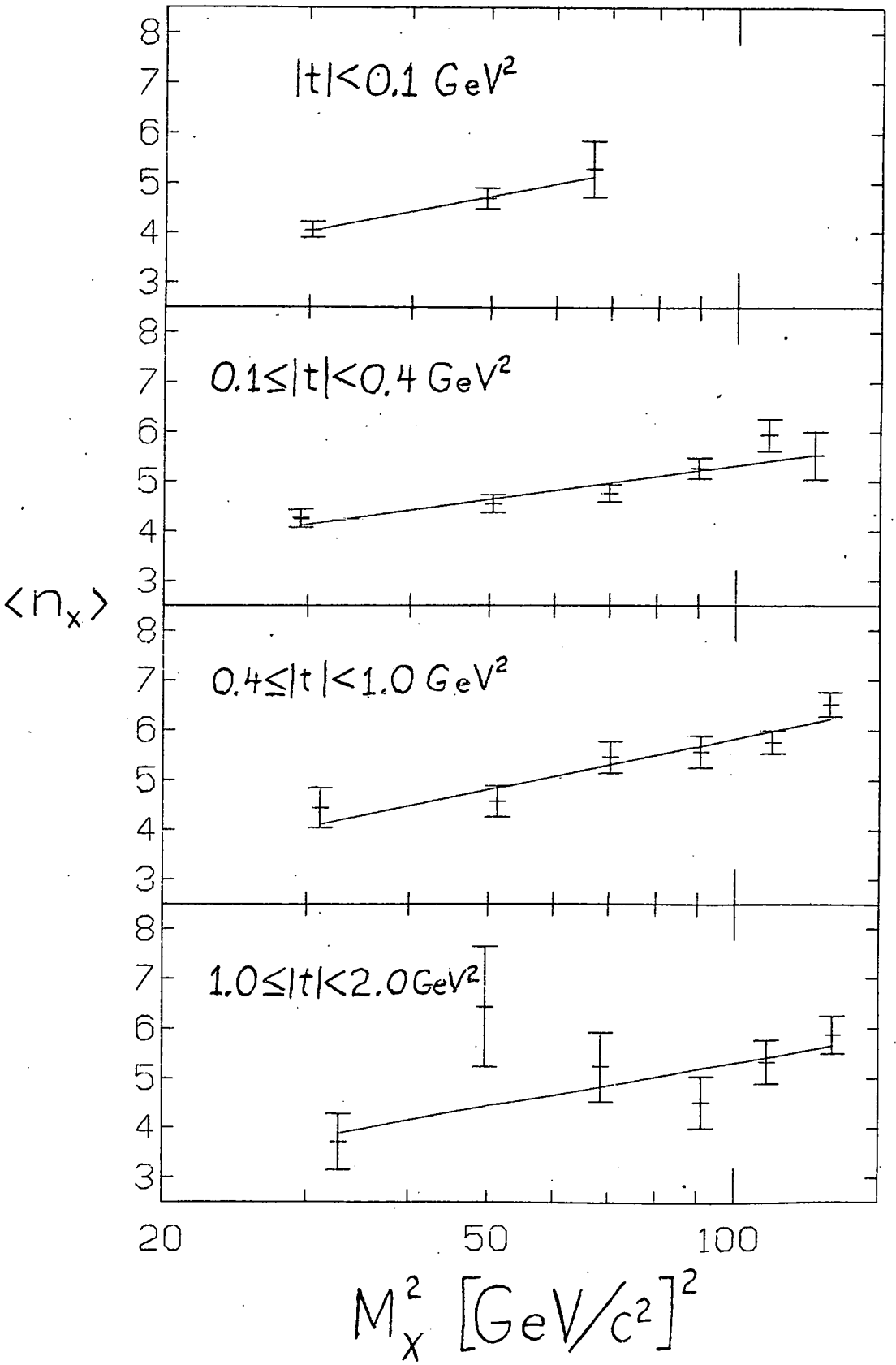

Fig. 2 (I a) i)

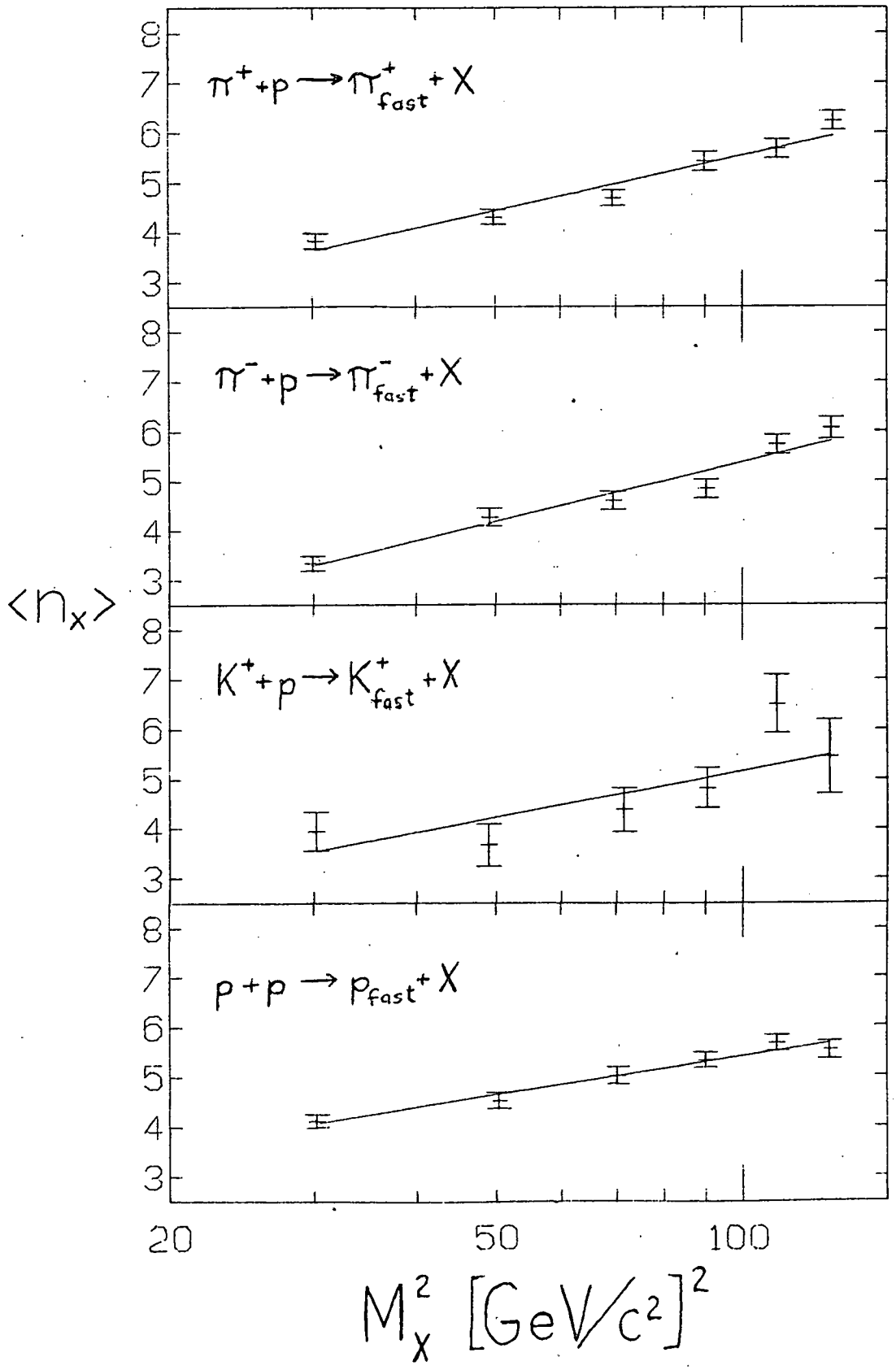
$\pi^+ + p \rightarrow \pi^+_{fast} + X$
$\pi^- + p \rightarrow \pi^-_{fast} + X$
$K^+ + p \rightarrow K^+_{fast} + X$
$p + p \rightarrow p_{fast} + X$
$\langle n_x \rangle$
3
4
5
6
7
8
20
50
100
M_x^2 [GeV/c²]²

Fig. 3 (I a) i)

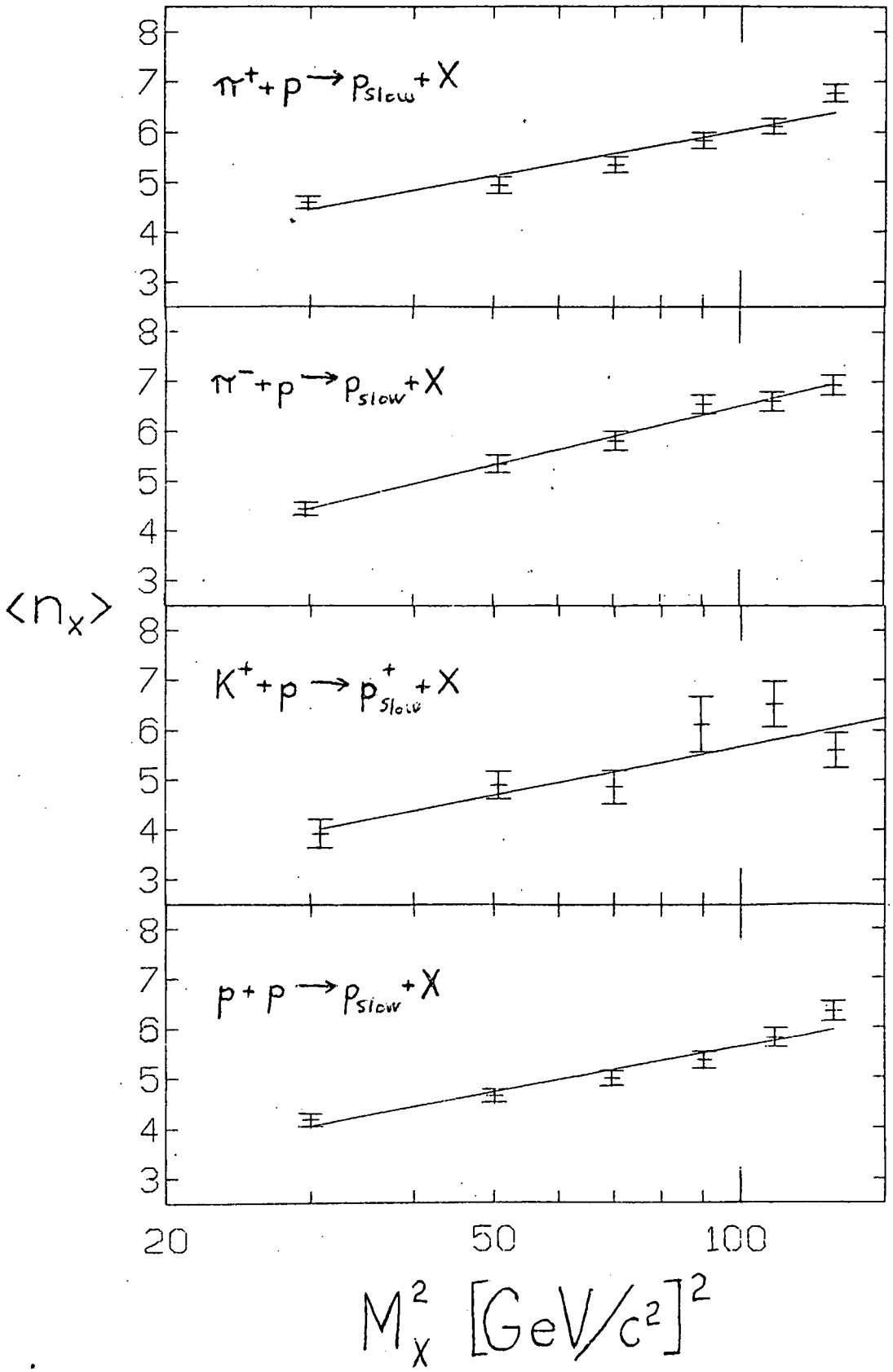
$\pi^+ + p \rightarrow p_{slow} + X$
$\pi^- + p \rightarrow p_{slow} + X$
$K^+ + p \rightarrow p^+_{slow} + X$
$p + p \rightarrow p_{slow} + X$
$\langle n_x \rangle$
8
7
6
5
4
3
20
50
100
M_X^2 $[GeV/c^2]^2$

Fig. 4 (Ia) i)

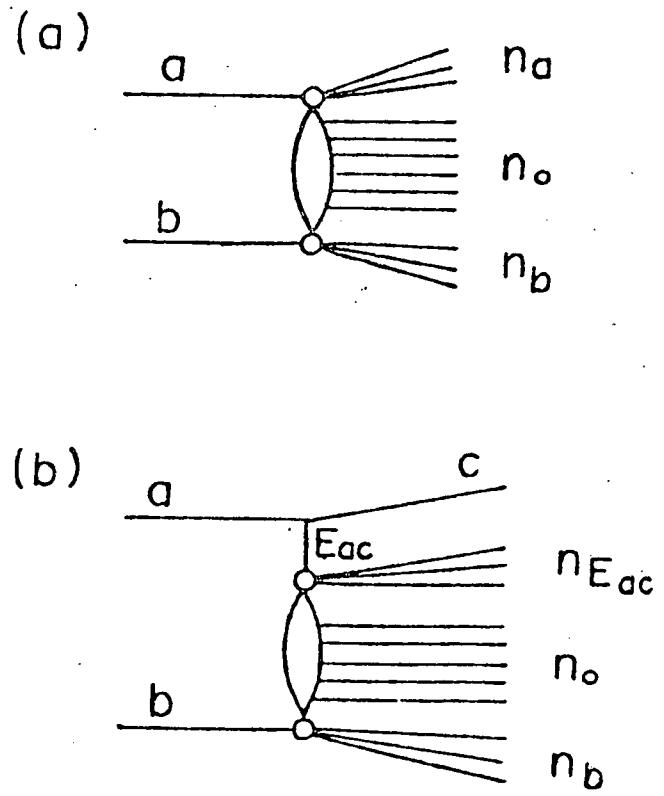

Fig. 5 (I a) i)

(ii) Clusters and High Transverse Momentum Jets.

The observed short-range rapidity correlations among particles in multi-particle events have been often interpreted in terms of the production of these particles through an intermediate stage called a cluster.[1]

The concept of clusters is related to that of the hadronic jets which have been observed in both e^+e^- collisions and hadron interactions. Although there is a commonly accepted method for analyzing hadron jets produced in e^+e^- interactions, an operational definition of jets in hadron-hadron interactions which produce hadrons is still needed. The problem of a "trigger bias"[2] is a well known example of how difficult it is to define a jet. A review of the methods used up to now can be found in Ref. 3.

The object of the present study is to assemble each event into groups of particles, clusters, which are somehow associated in full momentum-space, and not just in a one-dimensional space as in, for instance, the rapidity gap method.

We limit ourselves here to methods based on nearest neighbor techniques for associating particles into groups. First, we have to define a distance between any two particles of an event, each particle being regarded as a point in energy-momentum space. In our current study, three different metrics were tried as measures of the distance between particles in this space, each metric being related in a different way to the effective mass of the particle pair. Two different statistical algorithms[4,5] were applied for defining clusters, for each of the three distance metrics. Without going into further detail here on either the metrics or the algorithms, we will describe some of the results obtained with the various combinations of

metric and algorithm.

Each event was divided into clusters in 6 different ways (6 combinations of algorithm/distance), and the clusters were studied to see if they reproduced certain known cluster-type correlations previously found to occur in interactions of 147 GeV/c π^- with protons,[6,7,8] and to see whether the clusters identified by the different techniques have the same properties.

First, we compared the results of our paper[6] giving the central fireball cross-section as determined from a rapidity-gap analysis with our cross-section for events having 3 or more clusters. Two combinations of algorithm/distance are excluded on the basis of this comparison, as they give too low a cross section.

Second, our clustering methods should result in leading particles appearing in single particle clusters with cross-sections agreeing with those given in our paper, Ref.7. Thus, we applied the same cuts in Feynman x as in Ref. 7 to our 1-particle clusters and compared the results. It turns out that a third algorithm/distance combination gives rise to a proton leading cross section which is systematically too high.

Third, using only the events $\pi^- p \to 2\pi^- 2\pi^+ X^o$, and applying the same cuts as in Ref. 8 (to obtain off-mass-shell diffraction), we were able to reproduce the result of that analysis for the 3 remaining combinations of algorithm/distance. These included one representative of the algorithm described in Ref. 4, and two of the algorithm described in Ref. 5.

Some general properties of clusters produced by these three combinations were compared with each other and were found to be in agreement. The average number of clusters per event is found to be small, and increases with the multiplicity of the event by about 0.5 clusters per 2 prongs, starting from the ap-

proximate value of 2 clusters for the 4-prong events.

On the average, there are slightly less than 3 charged particles per cluster, and the distribution is always narrower than a Poisson distribution ($\sigma^2<2$). The invariant mass distributions of the clusters have no significant features.

A crucial point is whether or not the known resonance signals in the data remain intact when events are broken up into clusters. The familiar resonances do not seem to appear as isolated clusters (no ρ^o signal is seen in the invariant mass spectrum for two-pion clusters). In order to study known and well resolved resonances, we selected events having a Δ^{++} resonance (Δ^{++} has been defined by $1.12 \leqslant M(p\pi^+) \leqslant 1.32$ and $|t_{p\Delta}| < 1.$), and clustered these 389 events. The results are displayed in Table I for both distances, for the algorithm of Ref. 5. The main points to notice are the remarkable stability of the results against the choice of metric, and the small number of cases in which the p and π^+ of the Δ^{++} appear in different clusters, 3 for one of the metrics, 0 for the other.

The same kind of study cannot be done for the ρ resonance, because of the well known large combinatorial background. However, we know that some ρ's must be found in the beam diffraction dissociation component. So we present in Fig. 1 the $\pi^+\pi^-$ invariant mass spectrum, for π's belonging to the same cluster, this cluster having been chosen by the following procedure. In order to enrich the sample in beam diffraction dissociation, we took only two-cluster events, and computed the $\pi^+\pi^-$ invariant mass for the forward cluster, providing that its charge is -1 (charge of the beam) and its rapidity is greater than 1 (to remove the central region). A ρ signal is clearly visible in Fig. 1, for both distance measures, and is even more enchanced if we

select only the (3π) clusters (dashed histograms).

Another check is to examine the charge of the clusters, since it has to reflect the well-known local compensation of charge. We found that approximately 75% of the clusters arising from each of the three algorithm/distance combinations have a charge equal to 0 or ± 1.

The stability of the results against any particular choice of algorithm and/or distance suggests that the cluster structures are not created by the methods. Whatever dynamics underlies the pattern, the method provides an apparently meaningful prescription for reducing multiparticle events to few-body structures. It then becomes of interest to examine the kinematic properties of the clusters.

Figure 2 shows the invariant cross section, integrated over the whole rapidity range, for both single pions and clusters, as a function of the transverse momentum of these objects. The single particle distribution shows the expected exponential behavior, with perhaps a higher tail than that given by a pure exponential. The clusters coming from all three algorithm/distance combinations show a unique behavior. When compared with the single particle distribution, a crossover appeared at $p_T \sim 0.8$ GeV/c. Above 2 GeV/c, the cross section for cluster production is one order of magnitude higher than for single particle production, which is just the behavior expected for what are now called high p_T jets. In Figure 3, we present an average of the results of the three algorithms for the production at 90^o, and compare it both with a result from a calorimeter experiment[9] and with the theoretical prediction of Ref. 10. Our cluster results lie systematically lower than both theoretical and experimental jet results, by a factor of ~ 5 when compared with Ref. 10. This would be expected if our clusters were in fact similar to the high p_T jets, because our

clusters contain only charged particles and the jets also include neutrals. In fact, if we assume that in our clusters the neutral particles carry 15% of the total p_T of the jet, our cross section curve shifts to remove the factor of 5 difference.[11]

Monte Carlo simulations show that we cannot exclude the possibility that the observed high-p_T behavior is a statistical fluctuation, so we are not able definitely to identify our high-p_T clusters with jets. We can, however, compare the properties of these high-p_T clusters with those of experimental jets. For this purpose, we call any cluster with $p_T > 1.5$ GeV/c a jet.

We find the following:

1) The inclusive cross section for $\pi^- p \to$ jet + X is, at our energy, of the order of 10% of the total $\pi^- p$ cross section.

2) Only 10% of jet events have more than one high-p_T jet.

3) The probability for finding a jet in one event increases with the internal multiplicity of that event.

4) The mean number of clusters found in jet events is slightly higher (3.56) than in all events (2.86).

5) Figure 4a) gives the distribution in Θ^*, the polar angle (in the center-of-mass system) of the jet axis, and it is interesting to note that this is the first analysis showing high-p_T jets in the backward hemisphere from a π-beam experiment. One may compare our data with predictions of the Feynman-Field quark model[12] at our value of $x_2 = 2p_T/\sqrt{s}$ of 0.22.

The ratio

$$R = \frac{\sigma(\pi^- p \to \text{jet} + X)_{45^o}}{\sigma(\pi^- p \to \text{jet} + X)_{135^o}}$$

of relative cross sections for producing a jet at $\Theta^* = 45^o$ and 135^o respect-

tively, is found to be $R = 1.47 \pm 0.24$, which agrees within three standard deviations with the value of ~2.2 predicted by Ref. 12.

6) The experimental mean values of the charge of the jets (Fig. 4b) allow us to deduce the meson charge ratios as a function of θ^* (see Table II). Our results are seen to be in good agreement with the predictions of Ref. 12 also given in Table II.

The mean charged-particle multiplicity $\langle k \rangle$ of the high-p_T jets is found to be $\langle k \rangle = 3.45 \pm 0.17$, higher than the value of 2.74 obtained for all clusters, and the multiplicity distribution is narrower than a Poisson distribution.

7) The distribution in momentum components of the jet particles along the jet axis and transverse to it are in good agreement with results for hadron jets produced either by lepton processes or in hadron-hadron collisions.

Thus we have identified clusters of correlated particles in multiparticle events in a way that seems to be independent of choice of particular metric or algorithm. Among the clusters, those with high p_T have properties similar to those of high-p_T jets seen in counter experiments, and their observed structure is is consistent with the predictions of the quark model of Field and Feynman.[12]

REFERENCES

1. See, for example:
R. Diebold, Proceedings of 19th International Conference on High Energy Physics, Tokyo, 1978, and references therein.

2. M. Jacob and P. V. Landshoff, Nucl. Phys. B13, 395 (1976).

3. S. Nielsen, Ph.D. Thesis, Copenhagen, August 1978 (Niels Bohr Institute) (unpublished).
See also: M. Deutschmann et al., Nucl. Phys. B155, 307 (1979), where a simple algorithm is used to produce multiparticle systems. The CCHK (ISR) and PLUTO (PETRA) collaborations are also using algorithms with a distance between particles for analyzing their data (private communications).

4. T. Ludlam, Yale Report No. COO-3075-210 (March 1978).

5. J. P. Benzecri et al., "L'algorithme de Classification Ascendante Hierarchique," Internal report (unpublished) of the Laboratoire de Statistique Mathematique, Universite P. & M. Curie, Paris (1975).
The first idea of such an algorithm applied in high energy physics can be found in: T. Ludlam and R. Slansky, Phys. Rev. D16, 100 (1977).

6. I. A. Pless et al., "Inclusive and Semi-Inclusive Charge Structure in π^-p Multiparticle Production at 147 GeV/c," contribution to Tokyo Conference (1978) (unpublished).

7. D. Fong et al., Phys. Lett. 53B, 290 (1974).

8. F. Barreiro et al., submitted to Phys. Rev. Lett.

9. C. Bromberg et al., "Comparison of Hadron Jets Produced by π^- and p Beams on Hydrogen and Aluminum Targets," (Fermilab preprint 7000.260).

10. R. P. Feynman, R. D. Field and G. C. Fox, Nucl. Phys. B128, 1 (1977).

11. This percentage is very low, but this is because our experiment suffers

from the following bias. If the neutral particles carry 50% or more of the total p_T of a jet, we are not able to say, using only the charged information, if there is a high-p_T jet or not. We can see high-p_T clusters only if the fraction of p_T carried by the neutrals is small. This kind of bias is similar to the well known "trigger bias" in counter experiments (see Ref. [2]).

12. R. Field and R. Feynman, Phys. Rev. D15, 2590 (1977).

TABLE I: Production of Δ^{++} in Clusters

	Algorithm Ref. 5, Metric 2		Algorithm Ref. 5, Metric 3	
	No. of Evts	Cross Section (μb)	No. of Evts	Cross Section (μb)
Direct Δ^{++}	108	390 ± 37	88	315 ± 34
in a $(p2\pi)_{cl}$	180	638 ± 47	189	660 ± 48
in a $(p3\pi)_{cl}$	64	290 ± 36	70	294 ± 35
in a $(p4\pi)_{cl}$	26	112 ± 22	29	143 ± 27
in a $(p\geq 5\pi)_{cl}$	8	45 ± 16	13	77 ± 21
Total	386	1475 ± 75	389	1490 ± 75
p and π^+ in two diff. cl.	3	15 ± 9	0	—

Table II: Average Jet Charge $\langle Q \rangle$ and π^-/π^+ Ratios vs. Polar Angle of Jet.

	Polar Angle θ^*		
	45°	90°	135°
$\langle Q \rangle_{jet}$	-0.36±0.04	-0.15±0.02	0.26±0.03
$\frac{\pi^-}{\pi^+}$(exp.)	2.10±0.25	1.35±0.15	0.59±0.07
$\frac{\pi^-}{\pi^+}$(Ref. 12)	2.25	1.18	0.52

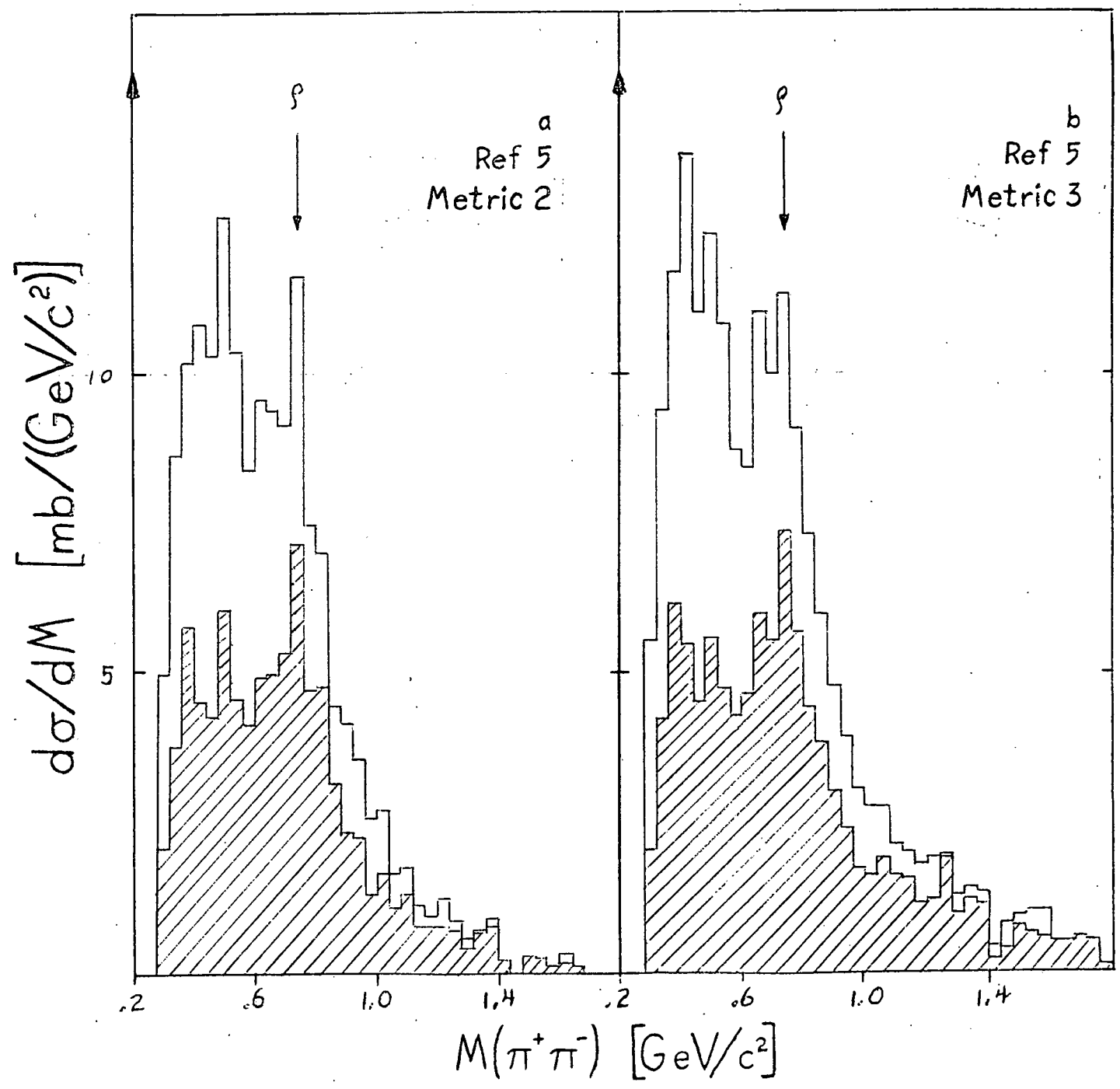
ρ
a
Ref 5
Metric 2
ρ
b
Ref 5
Metric 3
dσ/dM [mb/(GeV/c²)]
10
5
.2
.6
1.0
1.4
.2
.6
1.0
1.4
M(π⁺π⁻) [GeV/c²]

Fig. 1 (I a) ii)

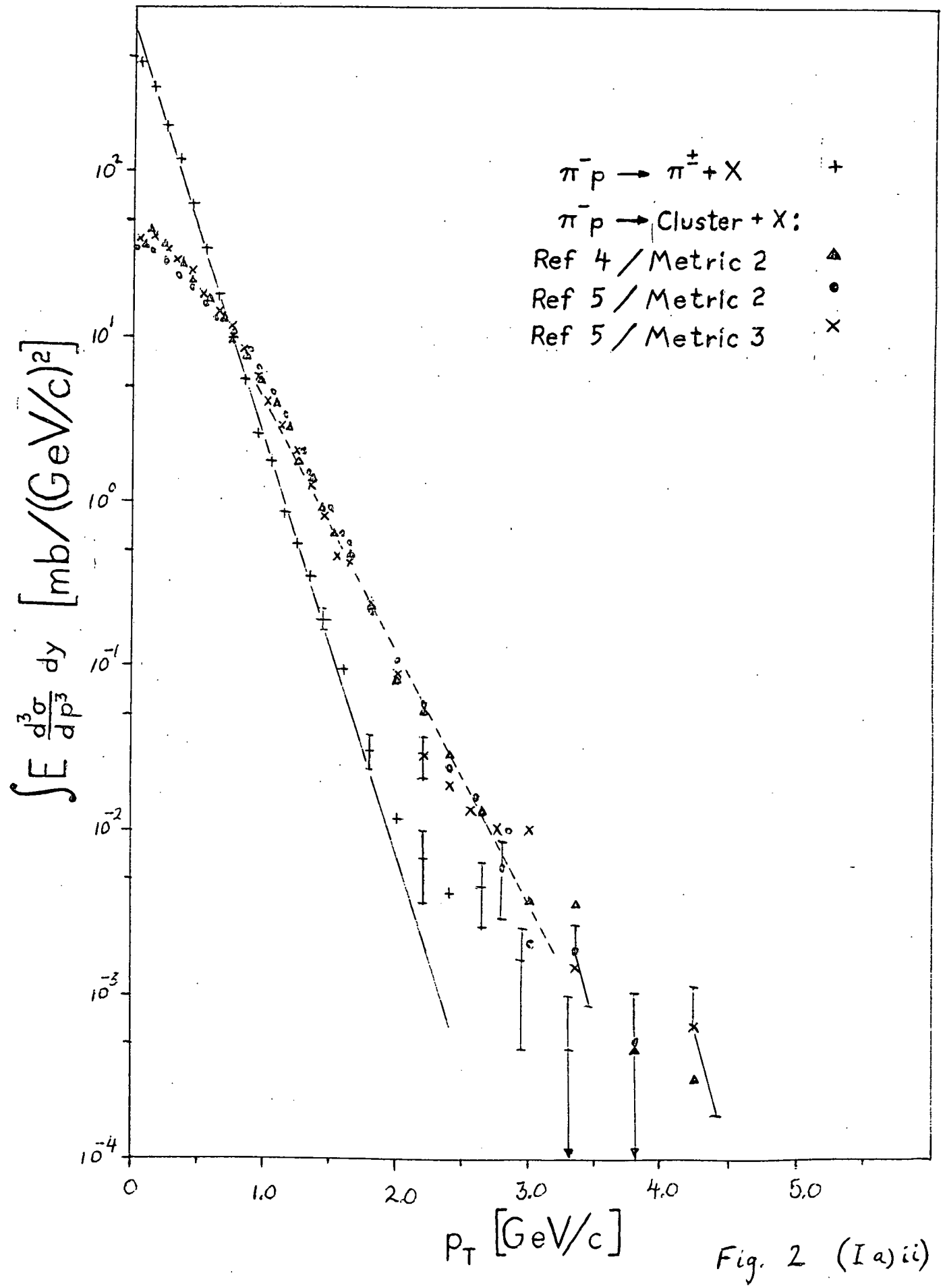
$\pi^- p \rightarrow \pi^{\pm} + X$ +
$\pi^- p \rightarrow$ Cluster + X:
Ref 4 / Metric 2 △
Ref 5 / Metric 2 •
Ref 5 / Metric 3 ×
$\int E \frac{d^3\sigma}{dp^3} dy$ [mb/((GeV/c)^2)]
10^2
10^1
10^0
10^{-1}
10^{-2}
10^{-3}
10^{-4}
0
1.0
2.0
3.0
4.0
5.0
p_T [GeV/c]

Fig. 2 (I a) ii)

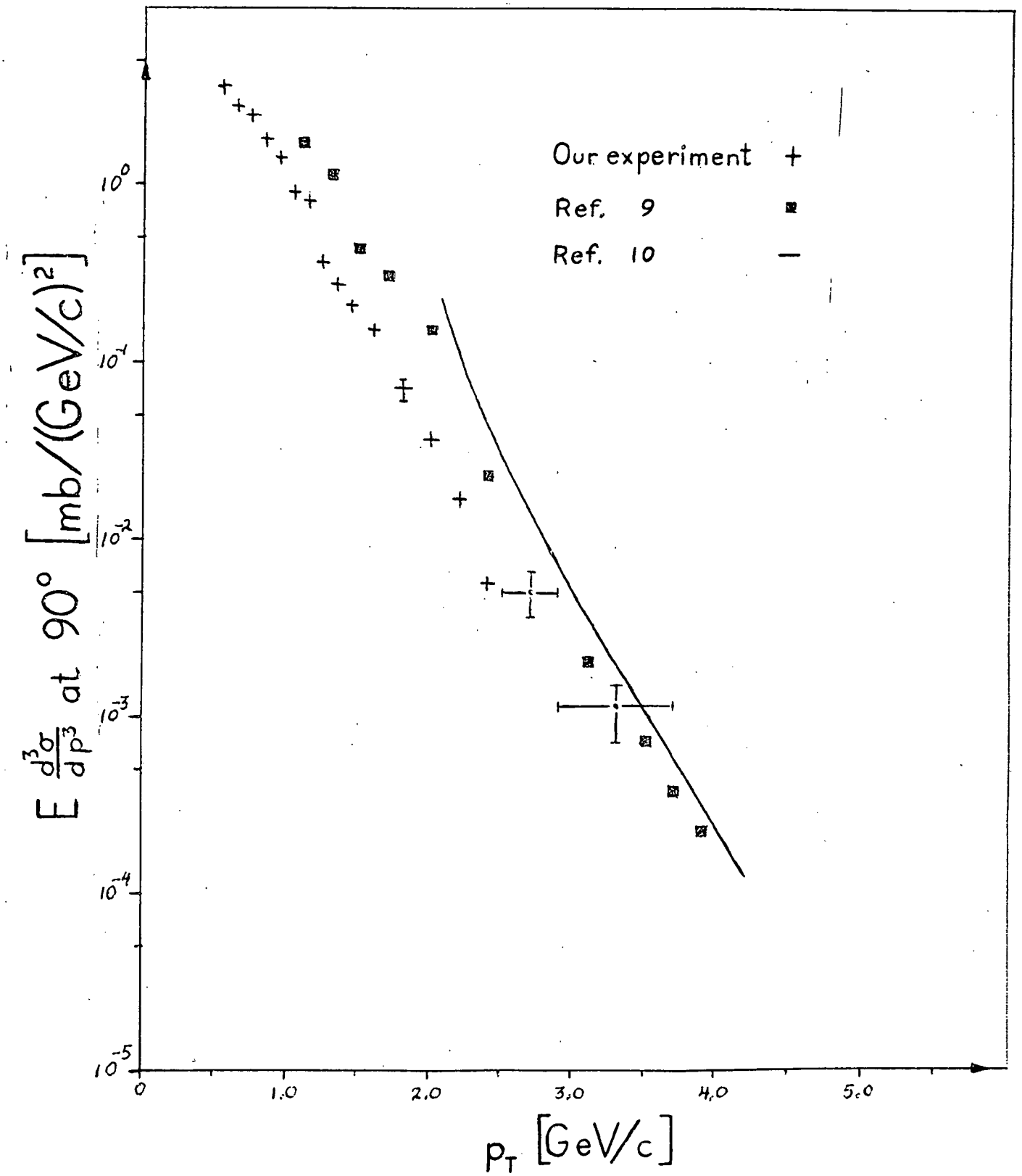
Our experiment +
Ref. 9
Ref. 10 —
$E\frac{d^3\sigma}{dp^3}$ at 90° [mb/(GeV/c)^2]
10^0
10^{-1}
10^{-2}
10^{-3}
10^{-4}
10^{-5}
0
1.0
2.0
3.0
4.0
5.0
p_T [GeV/c]

Fig. 3 (I a) ii)

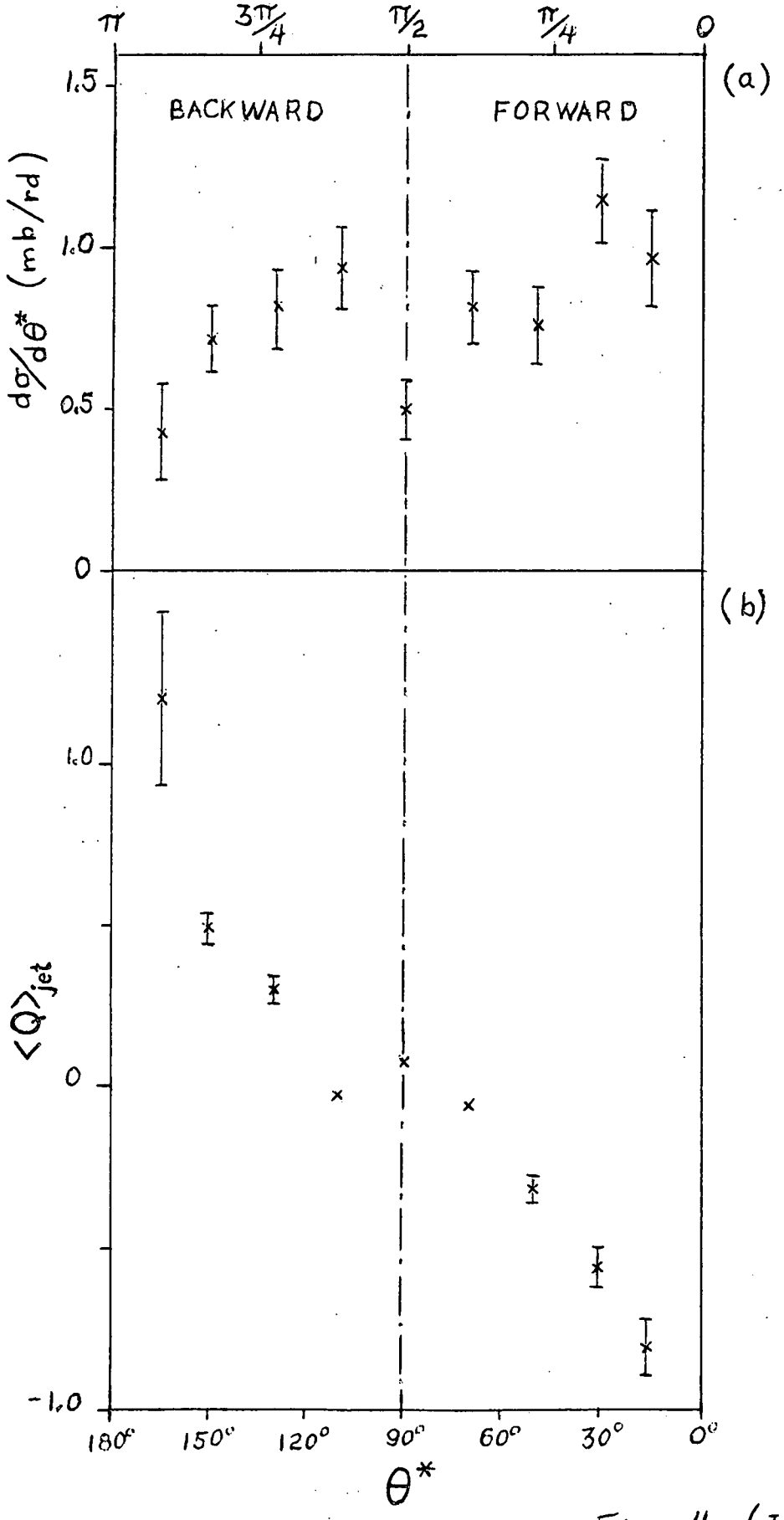
π
3π/4
π/2
π/4
0
(a)
BACKWARD
FORWARD
dσ/dθ* (mb/rd)
1.5
1.0
0.5
0
(b)
1.0
<Q>jet
0
-1.0
180°
150°
120°
90°
60°
30°
0°
θ*

Fig. 4 (I a) ii)

(iii) Production of ρ^o Mesons in $\pi^{\pm}p$, K^+p, and pp Interactions at 147 GeV/c.

A large fraction of all particles produced in high energy interactions are decay products of resonances[1,2] rather than directly produced, and the study of resonances can therefore yield more direct information about the basic processes of particle production.

The identification of these intermediate resonance states is a rather difficult task, especially at high energies. In this region difficulties arise from the large number of outgoing particles, leading to a significant combinatorial background, and from momentum resolution problems; the latter are minimized in the Fermilab Hybrid Spectrometer. In particular all the above problems hold for the production of vector mesons.

In the present work the cross section for ρ^o-meson production is determined in the following reactions:

$$\pi^+ p \rightarrow X^+ X^- \qquad (1)$$

$$\pi^- p \rightarrow X^+ X^- \qquad (2)$$

$$K^+ p \rightarrow X^+ X^- \qquad (3)$$

$$p\ p \rightarrow X^+ X^- , \qquad (4)$$

with X^+ and X^- being positive and negative particles, respectively.

The amount of ρ^o measured is very sensitive to the method of background description used; the present experiment has the advantage that all four reactions are treated in the same way, thus the differences in results for the different beam particle types might well be due to physical reasons.

To extract the cross sections from the invariant-mass distributions, we have parametrized our effective mass distributions with the following func-

tion:

$$F(m) = BG(m) + PS(m) \times BW(m)$$

where BG(m), PS(m), and BW(m) represent the background, the phase space, and a Breit-Wigner curve respectively. Assuming that the background and the two-particle phase space can be described by the same mass dependence, F(m) becomes:

$$F(m) = BG(m) \times (1 + BW(m)).$$

As background parametrization, a second order polynomial in the mass is used, and the shape of the ρ^o resonance was generated according to a p-wave Breit-Wigner with a central mass of 776 MeV, and a FWHM of 155 MeV. A Monte Carlo technique was used to include the correct mass dependent experimental resolution of the spectrometer. This function was fitted in the region between 0.55 and 3.0 GeV/c^2.

In Figures 1a, 2a, 3a, and 4a the effective mass distribution of the $\pi^+\pi^-$ system is plotted for the four different beams (reactions 1-4). The background parametrization is shown in the same figures. In Figs. 1b, 2b, 3b, and 4b the difference between the experimental mass distribution and the background is plotted. A clear signal is visible in all four cases.

The results of the topology dependent fits are given in Table I. The fits have an average χ^2/NDF of 1.2. For all incoming particles, the cross section for ρ^o production was normalized to the corresponding topological and total cross sections published earlier[3]. Uncertainties in the measured total cross sections were included in the errors. However, other systematic effects were not. The results of the fits are consistent as can be seen by adding the contributions of the fits for the different topologies and com-

paring the sum obtained to the direct result from the fit to the total inclusive distribution.

A comparison of the fits for the different beam particle types gives the following conclusions:

- At 147 Gev/c the number of ρ^o resonances produced per event is slightly larger in meson-baryon interactions than in proton-proton.
- ρ^o production per event increases with topology for all four reactions.

Using the same fitting procedure as described above, ρ^o production was determined as a function of the Feynman scaling variable x. The quality of these fits is comparable with the topology-dependent ones. It has been verified that the general shape of the x-dependence at large x, as opposed to the integrated cross section, does not depend on the background subtraction method used.

In Fig. 5, the invariant production cross section of ρ^o-mesons is plotted as function of x for the four reactions studied. In reaction (4) one should expect the contributions to be equal in the forward and backward hemisphere. The results seem to agree with this expectation, suggesting that no large systematic errors are made in either of the two hemispheres. The x dependence of $pp \to \rho^o$ and $K^+p \to \rho^o$ both appear symmetric, with large statistical errors on K^+p, while ρ^o production from $\pi^\pm$ appears much flatter in the forward than in the backward direction. The x dependence for reaction $pp \to \rho^o$ is the same as seen in the backward regions for $\pi^\pm p$ and K^+p reactions.

In spite of the large statistical errors involved, a study of the x-dependence of the directly produced ρ^o-meson is capable of verifying conclusions drawn from statistically more significant experiments which look at pion and kaon production only.[4,5] In Fig. 6, the forward hemisphere

distributions are plotted as functions of log(1-x). We have compared these distributions with the predictions of several theoretical models:

1. The dimensional counting rules (DCR) predict a $(1-x)^n$ dependence of the invariant cross section. The following functions have been fitted to the data in the interval $0.0 < (1-x) < 0.8$.

$$\frac{1}{\pi\sigma_{in}} \int dp_t^2 \frac{E^*}{\sqrt{s}} \frac{d^2\sigma}{dp_t^2\, dx} \approx x\frac{d\sigma}{dx} = N\,(1-x)^n \qquad (5)$$

and

$$\frac{1}{\pi\sigma_{in}} \int dp_t^2 \frac{E^*}{\sqrt{s}} \frac{d^2\sigma}{dp_t^2 dx} \approx x\frac{d\sigma}{dx} = N\,\sqrt{x}(1-x)^n \qquad (6)$$

The factor $\sqrt{x}$ in (6) is included to describe the x-dependence near $x = 0$, and can be neglected for large values of x. The values for the power n can be compared to the expectations in Reference 6. Considered together, the fitted n values are only consistent with the expected n=1 for $\pi^{\pm}p\to\rho^o$ and $K^+p\to\rho^o$, and n=3 for $pp \to \rho^o$, if $\sqrt{x}$ is included. The results of the fits using (6) are indicated in Fig. 6 with a dotted line.

2. The vector meson is assumed to originate from quark recombination (QRM).[4] A valence quark with momentum fraction x_v in the incoming particle picks up a sea quark, which has x_s near zero, to form the outgoing particle with $x = x_v + x_s$. The parametrization of this process is, for Mp and pp, respectively:

$$x\frac{d\sigma}{dx}(Mp \to \rho^o) = N\frac{(1-x)^{k-1}}{x}\int_o^x dy\; yF_v(y)\; F_s(x-y)\left[\frac{y(x-y)}{x}\right]^{k-1}, \qquad (7)$$

$$x\frac{d\sigma}{dx}(pp \to \rho^o) = N\frac{(1-x)^{2k-1}}{x}\int_o^x dy\; yF_v(y)\; F_s(x-y)\left[\frac{y(x-y)}{x}\right]^{k-1}, \qquad (8)$$

where $F_v(y)$ is the probability of finding a valence quark in the incoming hadron with momentum fraction y, F_s the distribution of the sea quarks, and $\left[\frac{y(x-y)}{x}\right]^{k-1}$ is the recombination function. For incident $\pi^{\pm}$ or K^+,

we used for $F_v(y)$ and $F_s(x-y)$:

$$yF_v(y) = \sqrt{y}(1-y)^k , \qquad (9)$$

and

$$F_s(x-y) = C_s[1-(x-y)]^n , \qquad (10)$$

with n fixed at 6.

For the case where a proton was the incident particle the valence quark distribution $yF_v(y)$ was taken from Field and Feynman.[7] Varying the value of n between 4 and 8 gave only very minor changes for the value of k. Changing the range of the fit from $0.2 < x < 1.0$ to $0.35 < x < 1.0$ changed the value of k at most one-third of a standard deviation. The values of k associated with ρ^o-production are consistently lower than the values obtained for pion and kaon production, even with the factor $\sqrt{y}$ included in equation (9);[4,5] but higher statistics are desirable. Curves based on these fits are shown in Fig. 6 as solid lines.

3. The outgoing meson is produced by quark fragmentation (QFM).[8] The production of resonances fragmenting from an incoming meson in this picture is described by:

$$x\frac{d\sigma}{dx} = N \int_x^1 dy\ F_v(1-y)\ (x/y)\ D(x/y), \qquad (11)$$

where F_v is again the valence quark distribution of the quarks inside the incoming meson and D is the quark fragmentation function. For F_v we used the Field and Feynman parametrization from Ref. 7 and for D(x/y) we took the expression derived by the same authors in Ref. 9. Curves based on fits to this model are plotted as dashed lines in Fig. 6.

In principle this picture does not contain any free parameters so we first calculated a χ^2 using the description of Ref. 9. This χ^2 was

not acceptable compared to the QRM results. The same result is found if we use (9) to describe the quark structure function of the mesons. From our data we conclude that the quark fragmentation function D(x/y) from reference 8 does not describe the production of vector mesons correctly, but gives a dependence that falls more rapidly with x than our data suggest.

A parametrization of D(x/y) that is more in agreement with our invariant ρ^o cross section is the one derived by Andersson et al.[10] Using this expression for D(x/y) we obtained values for χ^2 that are comparable with the ones resulting from the fits of the QRM. These results are plotted as dashed-dotted curves in Fig. 6. Of course higher statistics and other experiments are needed to confirm this result.

Similar work in pp interactions was not tried, because no satisfying parametrization for the fragmentation of a diquark into a vector meson is available at the moment.

REFERENCES

1. J. Bartke et al., Nucl. Phys. B197, 93 (1976).
M. Deutschmann et al., Nucl. Phys. B103, 426 (1976).

2a. G. Jancso et al., Nucl. Phys. B124, 1 (1977).

2b. M. Albrow et al., Nucl. Phys. B155, 39 (1979).

3. D. Brick et al., Contributed paper 616 to the XIXth International Conference on High Energy Physics, Tokyo (1978).

4. R. G. Hwa and R. G. Roberts, Z. Physik C1, 81 (1979).

5. ABCCLVW Collaboration, "The Fragmentation Spectra in K^-p Interactions at 110 GeV/c," Contributed paper to EPS Conference, Geneva, 27 June - 4 July 1979.

6. J. F. Gunion, "Short Distance Counting Rules for Low-p_T Fragmentation," preprint UCD-79-4.

7. R. D. Field and R. P. Feynman, Phys. Rev. D15, 2590 (1977).

8. A. Capella et al., Z. Physik C3, 329 (1980).

9. R. D. Field and R. P. Feynman, Nucl. Phys. B136, 1 (1978).

10. B. Andersson et al., Nucl. Phys. B135, 273 (1978).

Table I: Semi-Inclusive ρ^o Production (fitted above an exponential background).

a) $\pi^+ p \rightarrow \pi^+ \pi^- + X$

top	χ^2/NDF	$\langle \rho^o \rangle$	σ_{top}	$\sigma(\rho^o)$
4	81/ 92	0.26 ± 0.06	3.64 ± 0.09	0.94 ± 0.21
6	114/ 95	0.30 ± 0.06	4.19 ± 0.09	1.25 ± 0.23
8	118/ 95	0.59 ± 0.08	4.01 ± 0.09	2.36 ± 0.32
10	98/ 95	0.61 ± 0.11	2.94 ± 0.08	1.80 ± 0.33
$\geq$ 12	95/ 95	0.79 ± 0.16	3.36 ± 0.10	2.65 ± 0.54
$\leq$ 8	139/ 95	0.38 ± 0.04	11.84 ± 0.16	4.53 ± 0.43
all	117/ 95	0.43 ± 0.04	19.84 ± 0.22	8.58 ± 0.71

b) $\pi^- p \rightarrow \pi^+ \pi^- + X$

top	χ^2/NDF	$\langle \rho^o \rangle$	σ_{top}	$\sigma(\rho^o)$
4	99/ 87	0.16 ± 0.05	4.12 ± 0.10	0.65 ± 0.21
6	122/ 95	0.37 ± 0.07	4.47 ± 0.10	1.64 ± 0.33
8	81/ 95	0.48 ± 0.10	4.30 ± 0.11	2.07 ± 0.42
10	109/ 95	0.63 ± 0.15	3.09 ± 0.09	1.94 ± 0.46
$\geq$ 12	120/ 94	0.66 ± 0.23	3.21 ± 0.09	2.12 ± 0.75
$\leq$ 8	106/ 95	0.28 ± 0.04	12.89 ± 0.18	3.58 ± 0.46
all	111/ 95	0.39 ± 0.04	20.99 ± 0.25	8.10 ± 0.95

c) $K^+ p \rightarrow \pi^+ \pi^- + X$

top	χ^2/NDF	$\langle \rho^o \rangle$	σ_{top}	$\sigma(\rho^o)$
4	63/ 41	0.34 ± 0.16	3.41 ± 0.20	1.16 ± 0.54
6	82/ 68	0.13 ± 0.14	3.47 ± 0.20	0.43 ± 0.49
8	118/ 84	0.43 ± 0.20	3.28 ± 0.19	1.41 ± 0.67
10	75/ 83	1.09 ± 0.35	2.35 ± 0.17	2.55 ± 0.84
$\geq$ 12	74/ 83	1.53 ± 0.48	2.77 ± 0.19	4.23 ± 1.37
$\leq$ 8	135/ 94	0.29 ± 0.09	10.16 ± 0.34	2.93 ± 0.92
all	149/ 95	0.54 ± 0.10	16.98 ± 0.45	9.10 ± 1.67

d) $p p \rightarrow \pi^+ \pi^- + X$

top	χ^2/NDF	$\langle \rho^o \rangle$	σ_{top}	$\sigma(\rho^o)$
4	102/ 94	0.13 ± 0.04	6.29 ± 0.16	0.82 ± 0.25
6	76/ 95	0.23 ± 0.05	6.95 ± 0.17	1.60 ± 0.37
8	112/ 95	0.34 ± 0.08	5.78 ± 0.15	1.97 ± 0.45
10	94/ 95	0.69 ± 0.12	4.20 ± 0.13	2.89 ± 0.51
$\geq$ 12	112/ 94	0.90 ± 0.18	4.91 ± 0.15	4.44 ± 0.91
$\leq$ 8	93/ 95	0.23 ± 0.03	19.02 ± 0.28	4.36 ± 0.62
all	110/ 95	0.35 ± 0.04	31.62 ± 0.40	11.07 ± 1.13

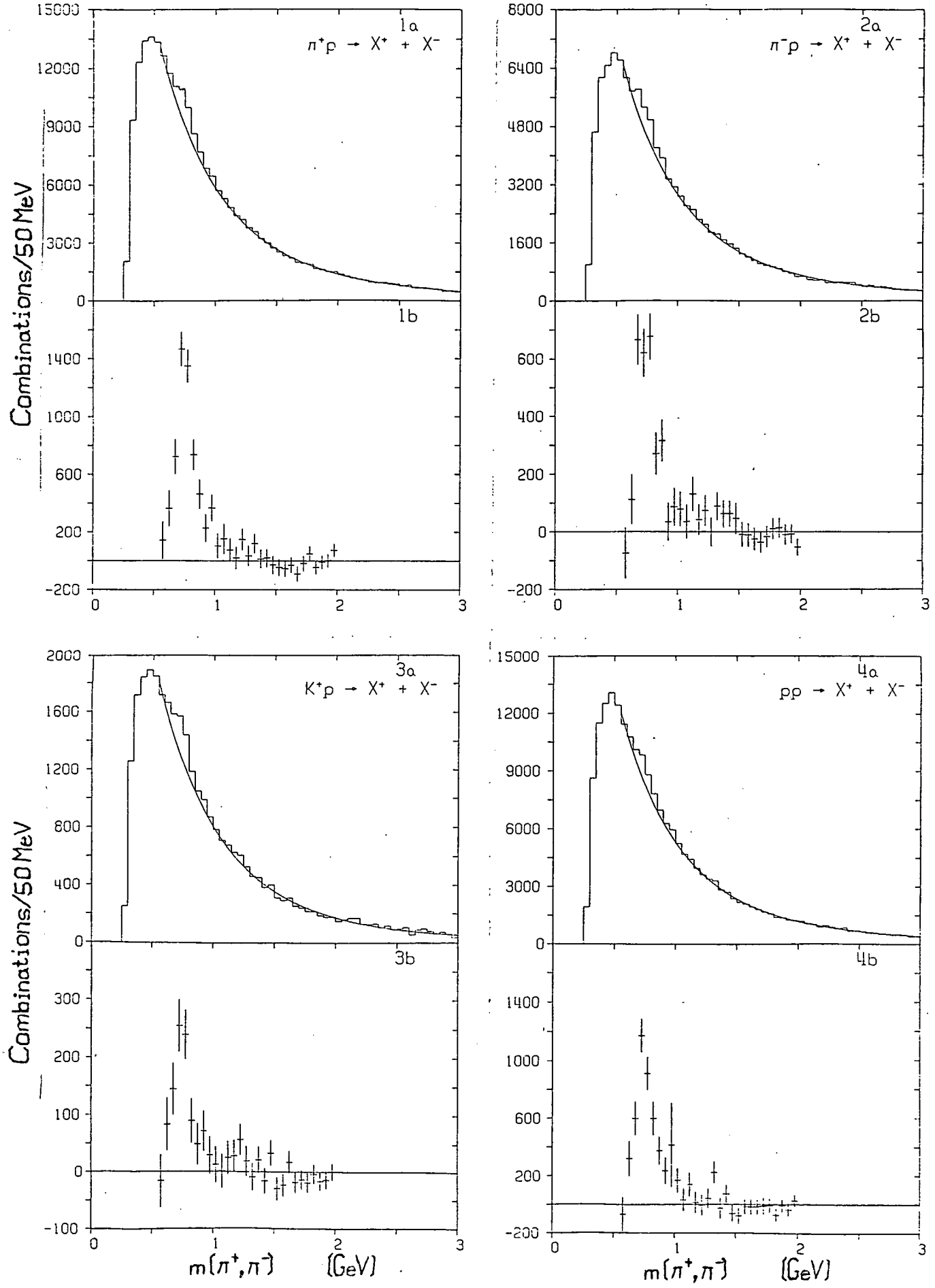

Fig. 1, 2, 3, 4 (I a) iii)

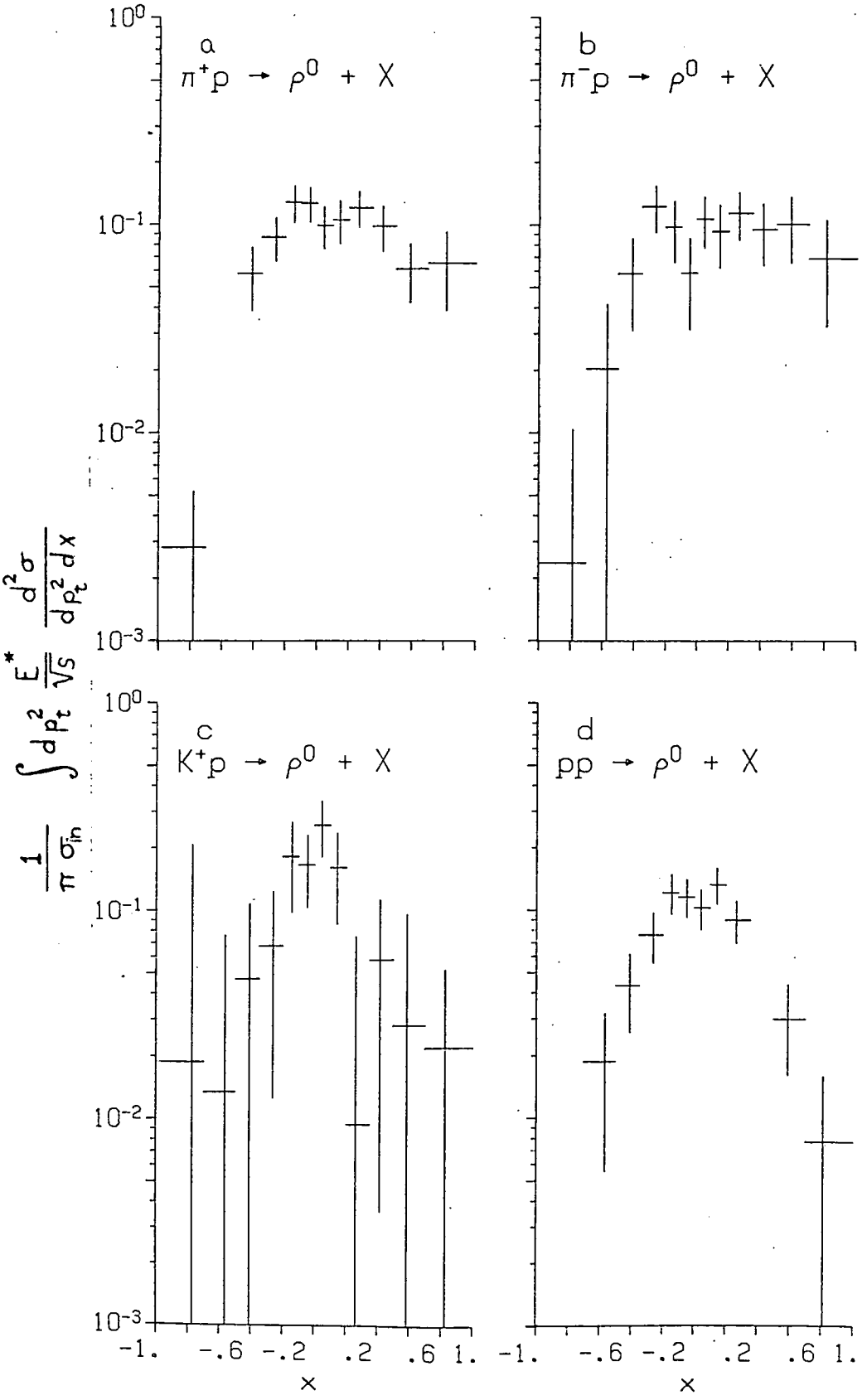
a
$\pi^+ p \rightarrow \rho^0 + X$
b
$\pi^- p \rightarrow \rho^0 + X$
c
$K^+ p \rightarrow \rho^0 + X$
d
$pp \rightarrow \rho^0 + X$
$\frac{1}{\pi \sigma_{in}} \int dp_t^2 \frac{E^*}{\sqrt{s}} \frac{d^2\sigma}{dp_t^2 dx}$
10^0
10^{-1}
10^{-2}
10^{-3}
-1.
-.6
-.2
.2
.6
1.
x

Fig. 5 (I a) iii)

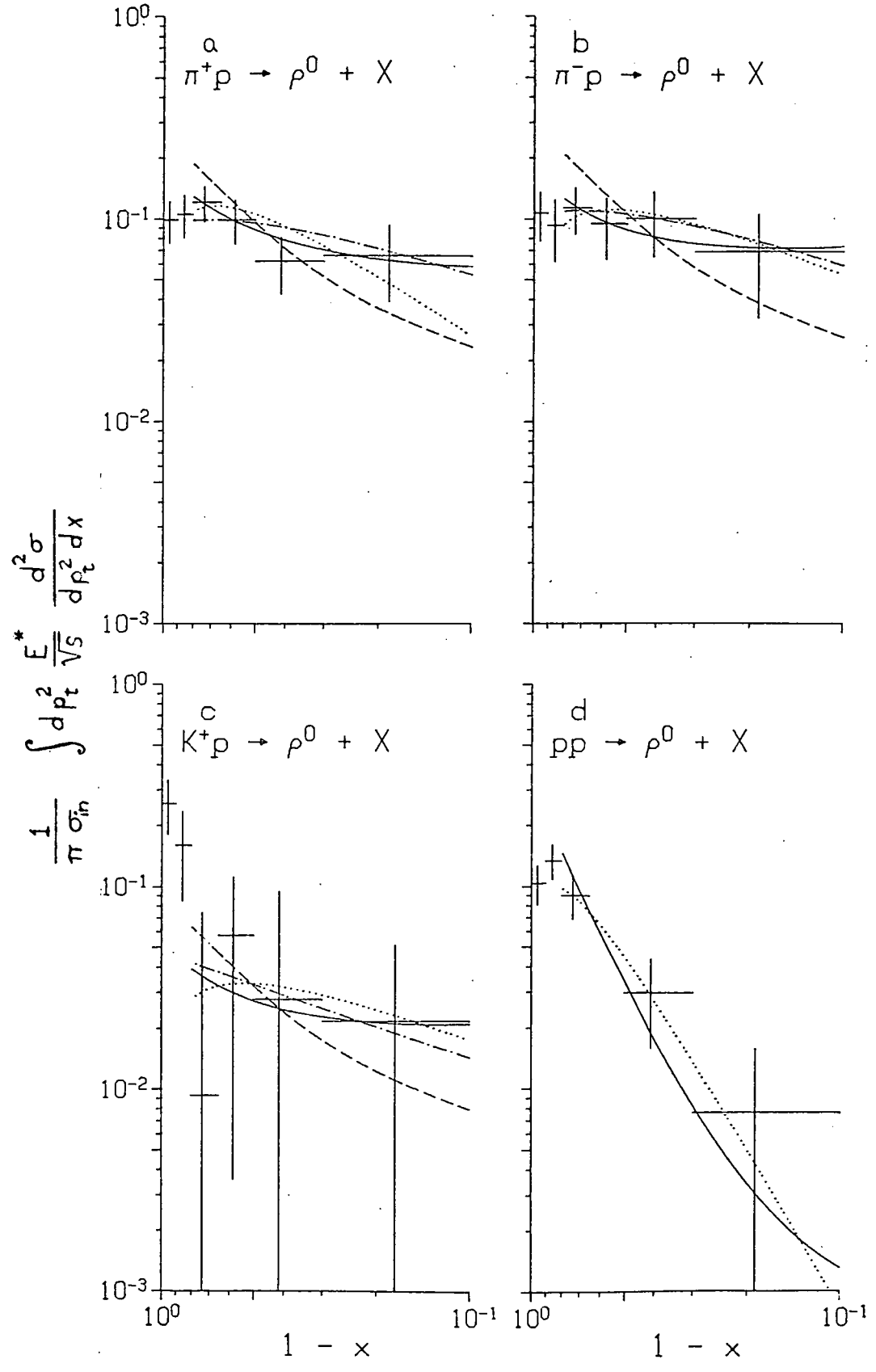
a
$\pi^+ p \to \rho^0 + X$
b
$\pi^- p \to \rho^0 + X$
c
$K^+ p \to \rho^0 + X$
d
$pp \to \rho^0 + X$
$\frac{1}{\pi \sigma_{in}} \int d p_t^2 \frac{E^*}{\sqrt{s}} \frac{d^2\sigma}{d p_t^2 dx}$
10^0
10^{-1}
10^{-2}
10^{-3}
$1 - x$

Fig. 6 (I a) iii)

b) The Argonne $\pi^+ p$ Bubble Chamber Experiment.

This experiment, studying $\pi^+ p$ interactions at 4.1 GeV/c in the Argonne (now FNAL) 30" chamber, has been performed by the Brown group as a secondary effort, with our main efforts being devoted to the Fermilab and SLAC experiments. Our analysis of the data is now complete and a final paper is being written.

To date, several papers have resulted from this work (References 154, 155, 163, 164, 173, and 194 in previous Progress Reports), three Ph.D. theses were completed earlier, and a fourth, by Martin Heller, was finished in the spring of this year. He has studied the one-constraint final state $p\pi^+\pi^o$.

The predominant quasi-two-body channels for this final state are:

$$\pi^+ p \rightarrow p\rho^+ \text{ and } \Delta^{++}\pi^o.$$

These channels are obscured, however, by the diffractive dissociation of the target proton, the $\Delta^+\pi^+$ channel, and general phase-space production of single π^o's, as well as misidentified cases of elastic scattering and multiple π^o production.

In order to be able to separate the competing channels as clearly as possible, a careful study of different techniques was begun. The prism-plot method developed by the MIT group[1] and the cluster-recognition method of Ludlam and Slansky[2] were investigated thoroughly. Of these, the former appeared to be better suited for the separation of three-body states. The final separation using the prism-plot method yields the cross sections listed in Table I. Also listed in this table are essentially all the results published on this reaction over the momentum range from 3.6 to 16 GeV/c. Our values are quite consistent with the general trends, but notice that there

are some wild fluctuations in the table for this relatively simple reaction. Clearly, more precise and definitive values are needed.

The best possible separation of the channels is important not only to determine the correct cross sections, but also for the detailed study of the dynamics of particular channels. Figures 1, 2, and 3 illustrate the separation of the channels by the prism-plot method, while Figures 4 and 5 show the differential cross sections and the decay matrix elements for the $p\rho^+$ and the $\Delta^{++}\pi^o$ channels, respectively.

A duality model of Harari's,[3] the dual absorptive model (DAM), appears to fit the characteristics of both of these reactions well, with vector mesons being exchanged in the t-channel. Rho-meson exchange appears to dominate the Δ^{++} production; and omega exchange appears predominant in the $p\rho^+$ reaction for momentum transfers > 0.01 $(GeV/c)^2$, while pion exchange is suggested at the lower momentum transfers. A final paper on this work is being prepared for submission to the Physical Review D.

REFERENCES

1. J. E. Brau et al., Phys. Rev. Lett. 27, 1481 (1971).

2. T. Ludlam and R. Slansky, Phys. Rev. D16, 100 (1977).

3. H. Harari, Annals of Physics 63, 432 (1971); Phys. Rev. Lett. 26, 1400 (1971).

Table I: A Comparison of Channel Cross Sections at Various Energies for the Reaction $\pi^+ p \to p\pi^+\pi^o$ (in microbarns).

Beam Momentum	Total σ	$p\rho^+$	$\Delta^{++}\pi^o$	$\Delta^+\pi^+$	Diff. Diss.	Phase Space	Ref.
3.6	2510±200	800±60	430±30				a
3.9	2300± 60	850±40	420±30	230±40	400±50	40± 20	b
4.0	2310	520±99	350±70			1550±310	c
4.1	2170± 40	900±30	276±16	123±19	257±16	615± 30	d
5.0	1300± 30	430±20	220±10	100±10			e
5.5			176±20				f
8.0	740± 60	141±10	110± 8				g
16.0	352± 5	59± 2	55± 2	25± 1	176± 3	1±0.3	h

a. J. MacNaughton et al., Phys. Rev. D15, 1832 (1977).

b. J. Brau et al., Phys. Rev. Lett. 27, 1481 (1971).

c. M. Aderholz et al., Phys. Rev. 138, B897 (1965).

d. This experiment

e. D. Schotanus et al., Nucl. Phys. B22, 45 (1970).

f. R. Bloodworth et al., Nucl. Phys. B81, 231 (1974).

g. M. Aderholz et al., Nucl. Phys. B8, 45 (1968).

h. M. Deutschmann et al., Nucl. Phys. B85, 31 (1975).

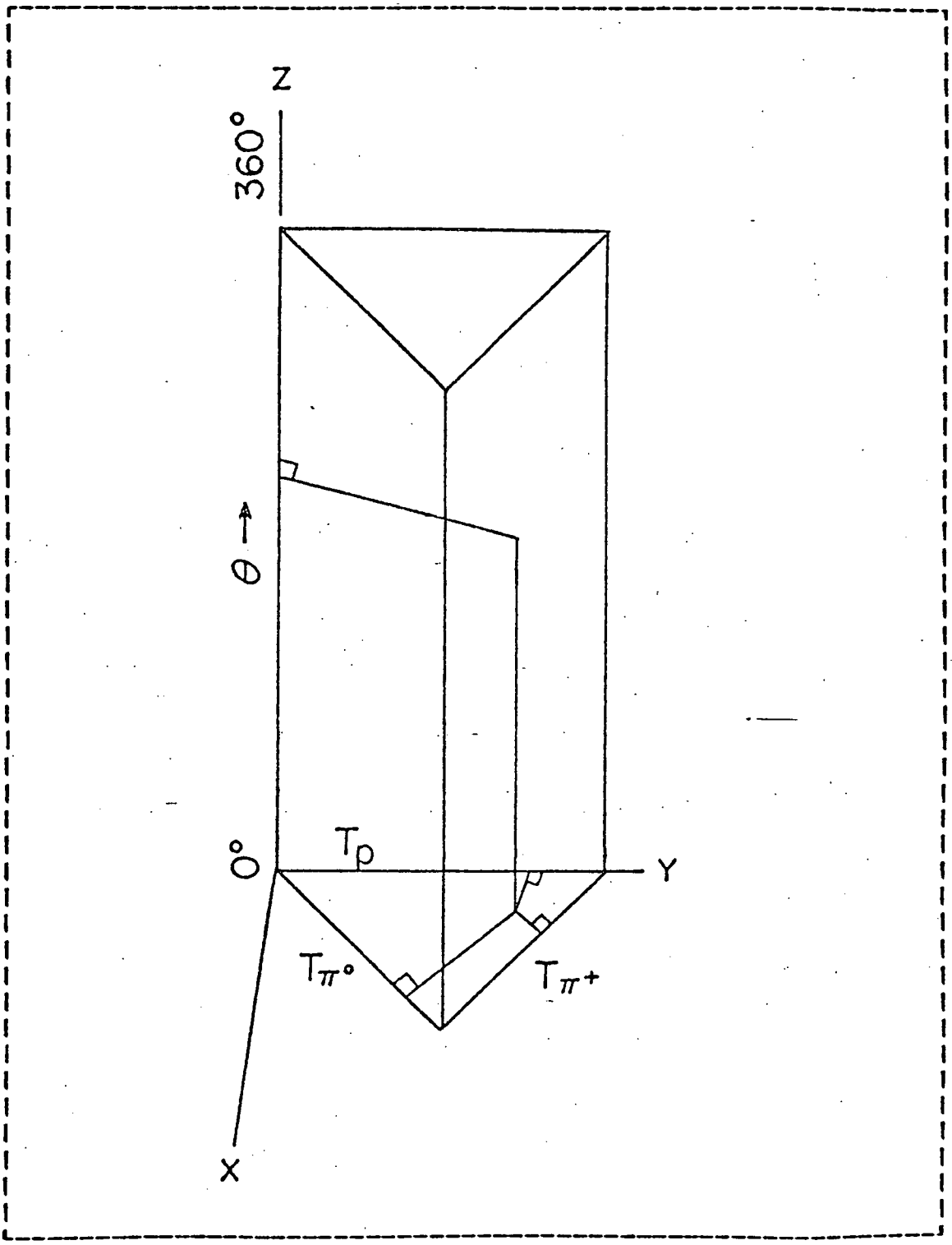

3-Body Prism Plot.
The figure shows how the Van Hove angle and the Dalitz-Fabri triangle are combined to make the 3-body prism plot.

Fig. 1 (Ib)

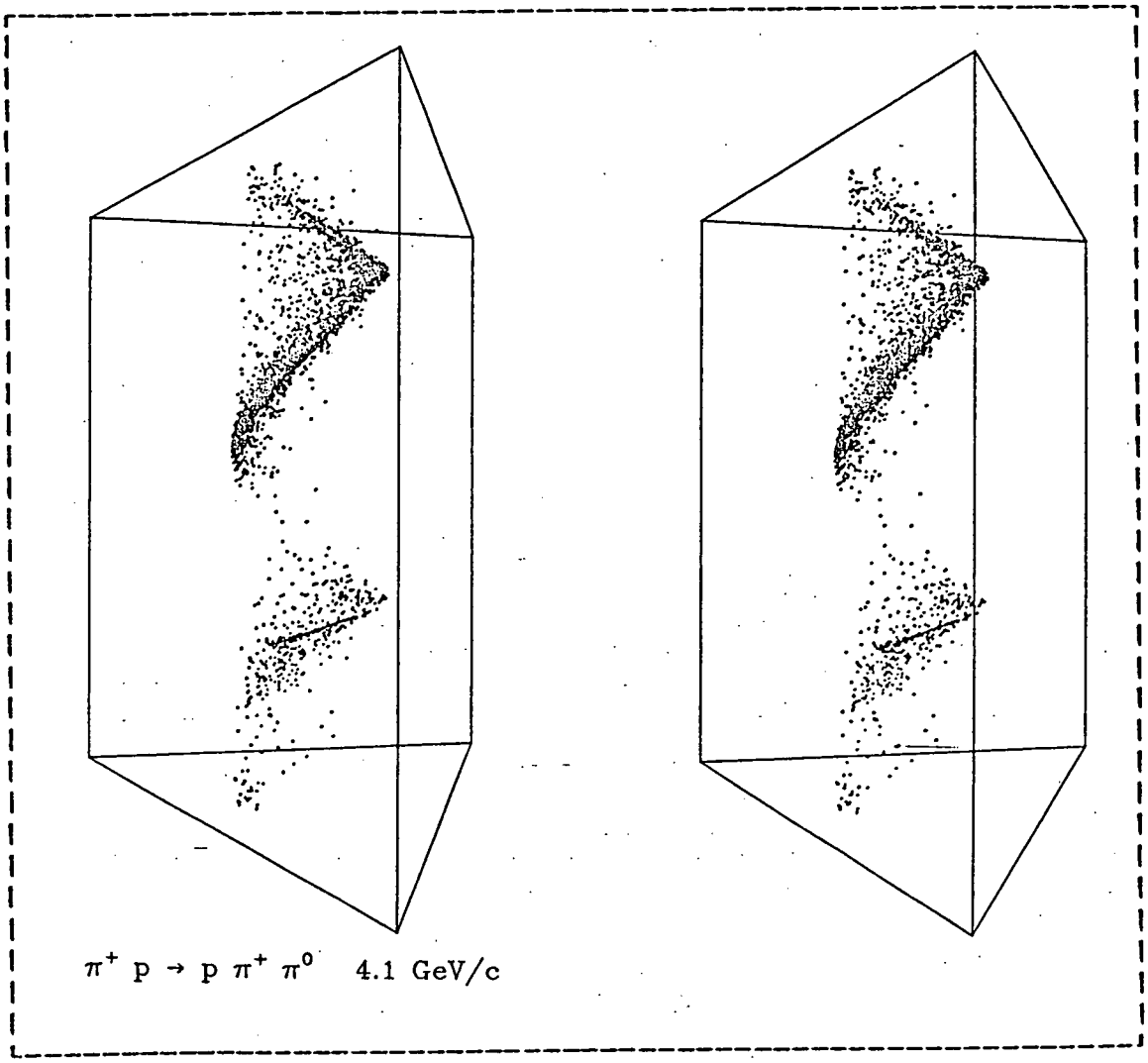

Prism Plot: 3154 Events.
This figure is a stereo pair, as is the succeeding figure. The prism-plot coordinates are defined in Figure 1. The separation of the events into a helix in this coordinate system is striking.

Fig. 2 (1b)

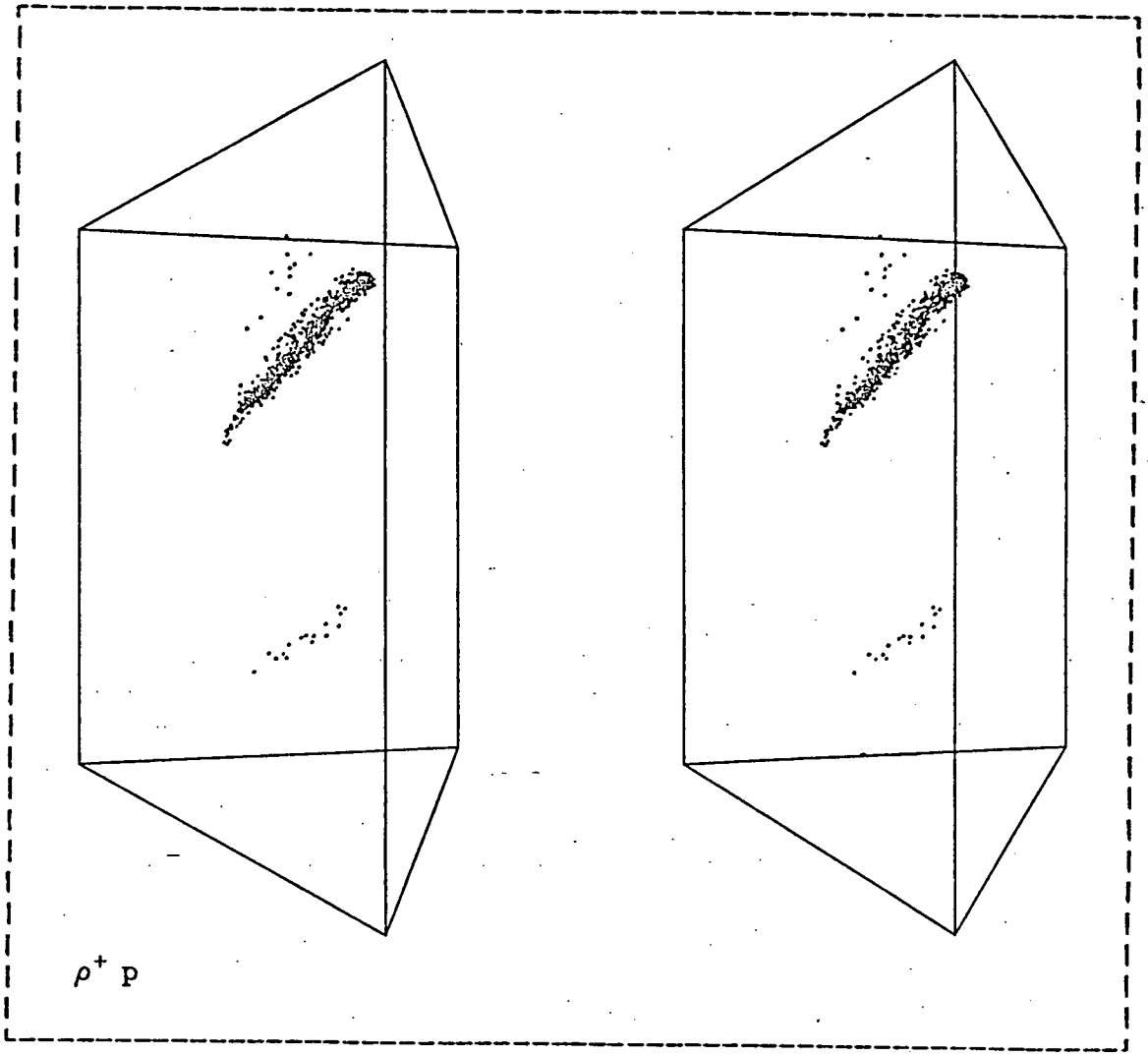

Prism Plot: Rho+ P.
The prominant dark tube is the forward rho+; the lighter tube near the bottom is the backward rho+. The few scattered events above and to the left of the main tube were probably improperly acquired by the rho+ channel.

Fig. 3 (Ib)

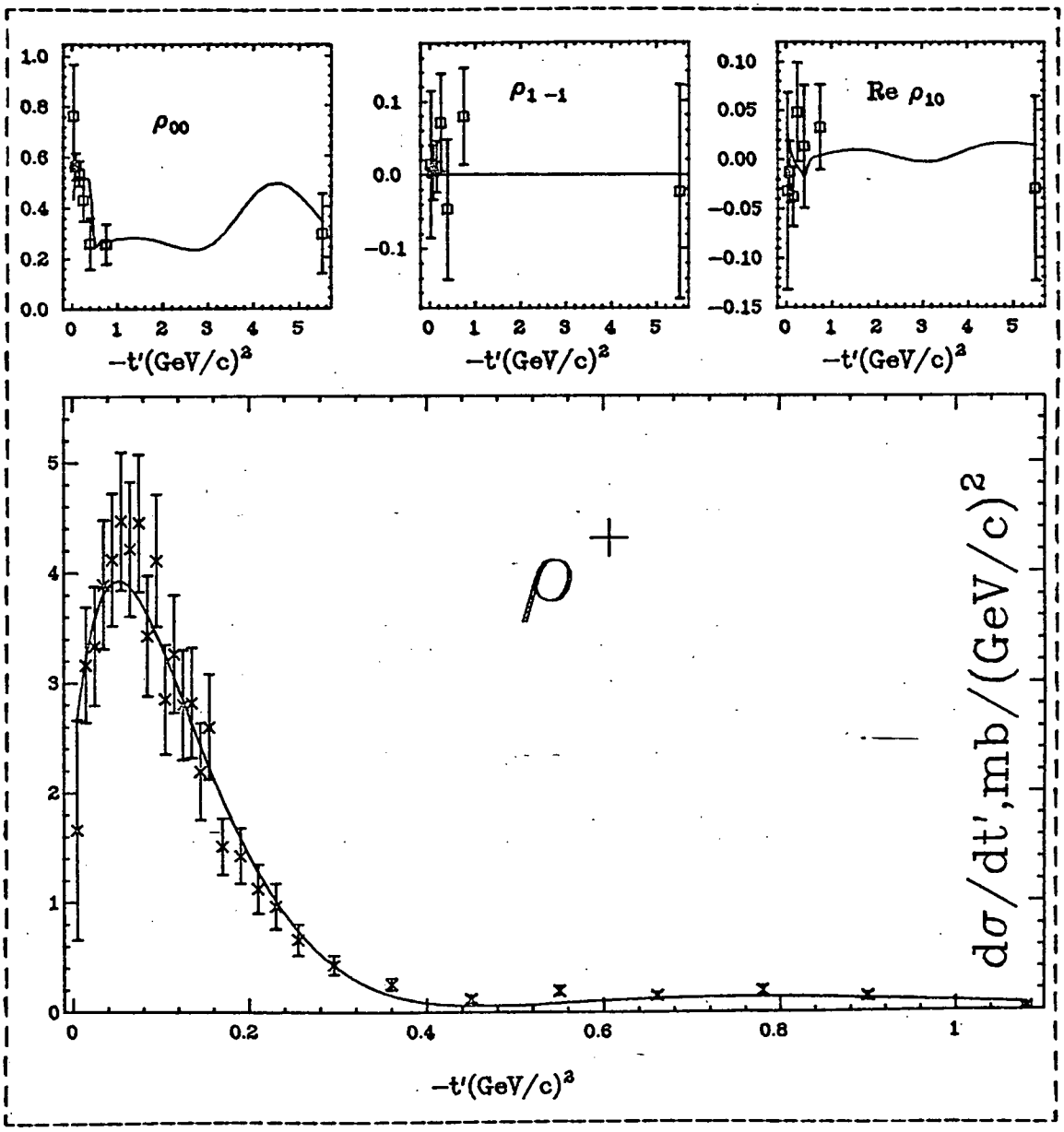

DAM Fit to Rho.
The figure shows a dual absorptive model fit to prism-plot-separated rho+ p events. The decay-density-matrix elements are shown across the top of the figure, and the differential cross section at the bottom.

Fig. 4 (Ib)

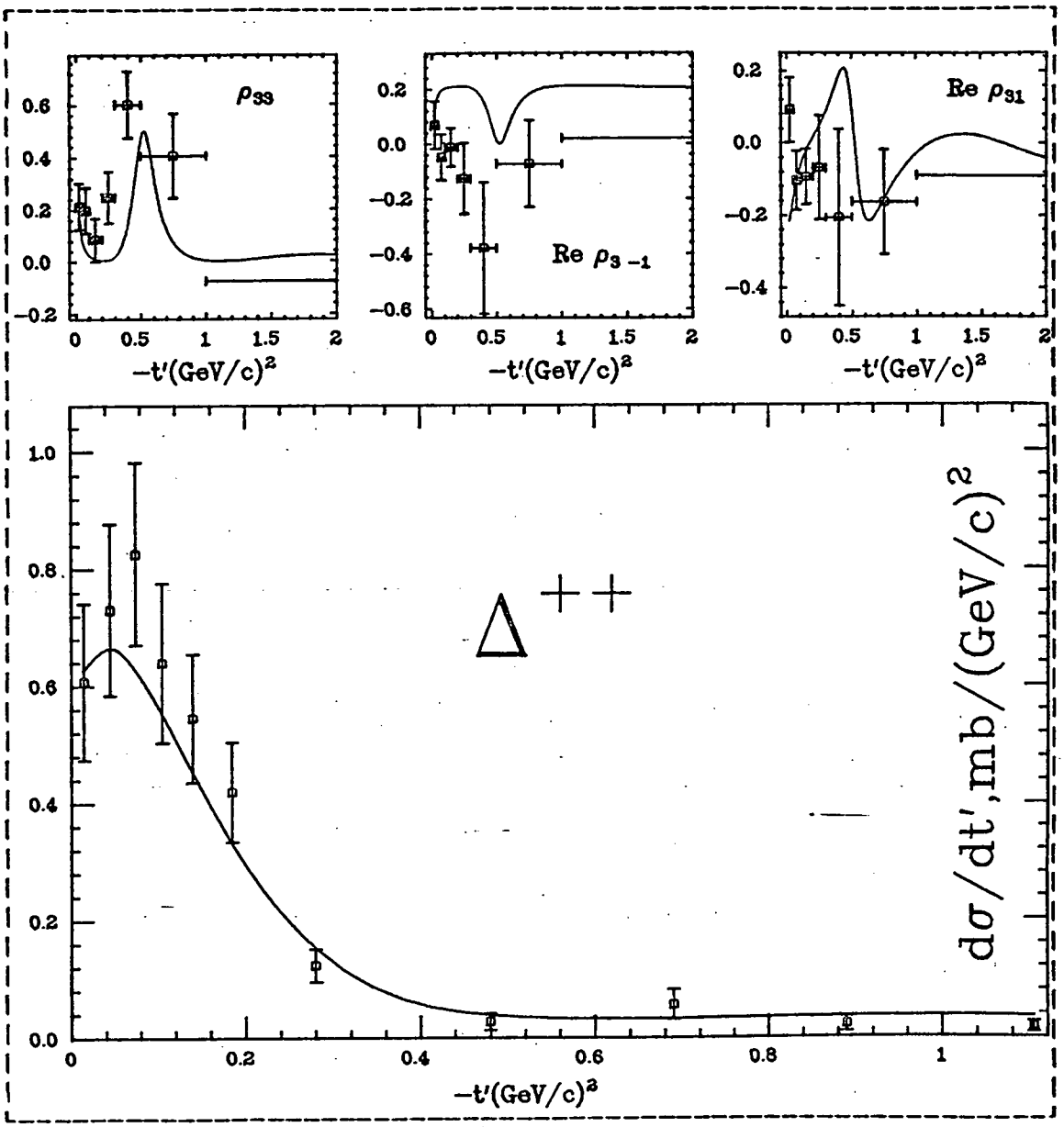

DAM Fit to Delta Differential Cross Section. The lower section of the figure shows the fit obtained with the dual absorptive model for the prism-plot-analyzed delta++ differential cross section. The upper sections show a comparison between the delta++ decay-matrix elements and the predictions of the theory.

Fig. 5 (Ib)

II. Experimental Runs in Progress and in Preparation.

(a) High Statistics Study of Particle Production and Dynamics From x=0 to x=1 and the Dependence on Incident Quantum Numbers (FNAL Experiment 570).

Experiment 570, which was approved in the spring of 1978, will be a comprehensive study of the dynamics of hadron production in hydrogen using five incident particle beams, $\pi^{\pm}$, K^{+}, p and $\bar{p}$, all at a momentum of 200 GeV/c.

The experiment is to be done using a hybrid spectrometer which is a more powerful version of the one used for E-154 and E-299. The major improvements include: (1) larger proportional wire chambers and drift chambers to provide a much larger solid-angle acceptance in the downstream portion of the spectrometer, along with a more precise determination of charged-particle trajectories; (2) the full scale 75 cm x 75 cm forward gamma detector; and (3) the CRISIS system which provides particle identification of secondaries with momenta between 5 and 50 GeV/c, by means of ionization sampling along the track.

The testing of the upgraded spectrometer in the beam which was scheduled to begin early in 1980 was first postponed and finally cancelled entirely by Fermilab, with our data-taking run now scheduled to begin in February, 1981. Wiring and cabling for the proportional wire chambers and drift chambers are in progress at Fermilab. Donovan Lewis and David Rossi, our technicians, have been spending time at Fermilab working on this.

The forward gamma detector has been at Fermilab since the full scale version was tested in 1977; it is essentially ready to run.

A 1m x 1m x 1m module of the CRISIS system was constructed and tested successfully in 1977; the system for the new spectrometer is a single

3m x 1m x 1m module, which has been completely constructed and assembled at MIT. Anatole Shapiro spent one half of his sabbatical year at MIT working on the design and construction of the gas system for CRISIS. The original test module used pre-mixed gases which flowed through the system and were exhausted to the atmosphere. Since this procedure would be too wasteful for a long run, a recirculating system was designed, built and tested. This apparatus provides precise control of the gas pressure, precise monitoring and adjustment as needed of the ratio of carbon dioxide to argon in the mixture, and continuous monitoring and removal of any oxygen.

The complete CRISIS has been tested at MIT using a radioactive source. It will be moved to Fermilab during the autumn, and beam time has been promised for further testing before the data-taking run begins in 1981.

The new spectrometer system will allow us to study in detail the production dynamics of particles and resonances, particularly in the central region, as a function of the quantum numbers of the projectile particles. Dependence on the quamtun numbers may be a direct consequence of the distribution of quarks in the incident channels, and thus can give information on the structure of the interacting particles, as well as on the dynamics of the collisions.

Almost all charged secondary particles produced with momenta between 5 and 50 GeV/c will be identified in the downstream CRISIS system, which takes many samples of ionization along particle tracks, providing identification in the region of relativistic rise in ionization. At the same time, the drift chambers and proportional wire chambers of the hybrid system provide excellent measurements of the directions and momenta of the particles. Also neutral particles decaying into forward-going gammas, and other particles and resonances decaying with one or more forward gammas, will have their

directions and energies precisely measured by the Forward Gamma Detector. Many V^o's (Λ^o, $\bar{\Lambda}^o$, and K^o_s) will also be identified and measured in either the bubble chamber or the downstream chambers or both. The bubble chamber, of course, provides vertex detection, with 4π coverage for charged particles. Hence almost all particles produced, both charged and neutral, particularly in the central region, will be well identified and measured.

Some of the specific physics topics to be investigated are listed below and are described in somewhat more detail in the accompanying Renewal Proposal.

(i) Single-particle distributions for identified charged and neutral particles.

(ii) Multiplicity studies, in reactions of the type $a + b \rightarrow c + X$, where a and c take on many identities in this single experiment, as well as in interactions of the type $a + b \rightarrow X$.

(iii) Correlation studies, including the question of neutral-charged particle correlations about which little is known. Questions of local conservation of transverse momentum, strangeness and other quantum numbers will be checked in a definitive way, not possible when only charged particles are identified. Cluster analysis will be pursued and the relation between hadron clusters and jets further investigated.

(iv) A systematic study of resonance production in the inclusive reactions:

$$\begin{pmatrix} \pi^{\pm} \\ K^{+} \\ p^{\pm} \end{pmatrix} + p \rightarrow \begin{pmatrix} \eta^o \\ \rho^{\pm}, \rho^o \\ K^{*\pm}, K^{*o} \\ \phi^o \\ \omega^o \\ \Delta^{++}, Y^* \end{pmatrix} + X \ .$$

Of these reactions, only those leading to ρ^o and Δ^{++} have been studied in any detail at Fermilab energies. The connection of resonances with clusters will be clarified.

(v) Four-constraint fits extended to events with one, two, and even three π^o's and events with charged K's.

(vi) Investigation of the large amounts of forward-going neutral energy observed in our experiment E-154 in low multiplicity events.

In addition, some more spectulative areas include:

(vii) A search for a possibly new phenomenon where both projectile and target end up near x = 0.[1]

(viii) A Search for charm and other new particles that decay into one or more heavy particles and several pions. This will be facilitated by the possible addition of a high resolution camera in one of the four camera ports.

(ix) A study of pairs of identical heavy particles to compare with the Bose-like behavior seen in identical pion-pairs.

Our Consortium, expanded to the International Proportional Hybrid System(IPHS) Consortium upon the addition of several European, Israeli, and Japanese groups, will run Experiments 570 and 565 concurrently during the spring of 1981. We are hoping to obtain about 1.5 million pictures in this run.

The first million pictures will be taken using a tagged positive beam of 200 GeV/c momentum, composed of approximately 10% K^+, 45% π^+, and 45% p. The next 0.5 million pictures will be taken with a tagged 200 GeV/c negative beam, enriched to about 20% $\bar{p}$ and with 80% π^- and perhaps a few percent K^-. Thus we shall be able to study the topics of interest with high statistics and will be able to make intercomparisons with minimum systematic errors.

We expect that definitive, precise new data will be produced by these experiments, and that unexpected phenomena may be uncovered.

(b) A Study of the Detailed Characteristics of Hadron-Nucleus Collisions Using the Fermilab Hybrid Spectrometer (Fermilab Experiment 565).

This experiment has been approved to run concurrently with E-570. We are planning to study with precision the dependence on incident particle, energy, and target of multiparticle production in hadron-nucleus collisions. Thin metallic foils of aluminum, silver and gold placed in the upstream region of the 30-inch chamber will be used as targets in addition to the hydrogen and the hybrid bubble chamber spectrometer with the downstream particle identifier will be used as the detector. These thin metal foils for E-565 will not interfere with the other experiment; interactions will occur in either the foils or the liquid in the chamber. For E-565 particularly, a beam of protons at 400 GeV/c or higher will be sent through the bubble chamber for a few hundred hours at the end of our run, in order to study the energy dependence.

Previous experiments[2-5] have indicated that the nucleus provides a powerful tool for the study of strong interactions, particularly for the investigation of the nature of the state of hadronic matter that exists between the instant of collision of two hadrons and the final production of particles. Many efforts have been made to interpret the general features of multiparticle production in hadron-nucleus interactions in terms of quark-parton models; at present, existing data are inadequate to distinguish among these models.[6-9]

For each incident particle and energy, the A dependence of the average multiplicity and the rapidity distributions of outgoing particles will be

investigated. The hybrid system will provide 4π coverage, good spatial resolution of tracks, good momentum measurements up to the highest energy, as well as particle identification of secondary pions, kaons and protons. The visual observation of the interaction vertex in the bubble chamber will keep systematic errors at a minimum, allowing a one-percent determination of multiplicities. This is essential for a definitive test of the models which have been developed. The hybrid spectrometer will measure the true rapidity distribution of the secondary particles, unlike other experiments which have yielded only the pseudo-rapidity.

In addition, it will be possible to detect and study the decays of associated strange particles as a function of A. This will be the first comprehensive study of this subject.

This experiment is described in more detail in the accompanying Renewal Proposal.

References for E-570 and E-565

1. M. Jacob, private communication.
2. W. Busza et al., Phys. Rev. Lett. 34, 838 (1975).
3. M. Binkley et al., Phys. Rev. Lett. 37, 571 (1976).
4. D. C. Hom et al., Phys. Rev. Lett. 37, 1374 (1976).
5. L. Kluberg et al., Phys. Rev. Lett. 38, 670 (1977).
6. B. Anderson, Proceedings of the VIIth International Colloquia on Multiparticle Reactions, Tutzing (1976).
7. A. Krzywicki, Proceedings of the Topical Meeting on Multiparticle Production from Nuclei at Very High Energies, Trieste (1976).
8. S. J. Brodsky et al., SLAC-PUB-1930 (1977).
9. A. Capella and A. Krzywicki, Phys. Lett. 67B, 84 (1977).

(c) Charm and Vector Meson Photoproduction in a Polarized Monoenergetic Backscattered Laser Beam of 20 GeV. (SLAC Experiments BC 72 and BC 73)

These experiments employ the SLAC Hybrid Facility (SHF) in a monoenergetic beam of 20 GeV photons. In BC 73 a high resolution camera is used in addition to the three conventional cameras of BC 72, to improve the separation of secondary vertices close to the primary vertex and hence to facilitate the search for charmed particles.

Major topics of interest in these experiments include:

1. A search for charmed mesons and baryons.

2. A high statistics study of vector mesons.

3. Spin-dependent effects in the inclusive production of Λ's and vector mesons.

4. Photoproduction of baryonium.

During the fall and winter of 1979-80, the SHF was moved to the backscattered laser beam site. The photons entering the SHF are essentially monoenergetic (20 GeV, with $\Delta E/E = 5\%$) and polarized. The SHF is shown in Fig. 1. It contains the following elements:

(i) The SLAC 40" bubble chamber filled with hydrogen.

(ii) Proportional wire chamber stations α, β, γ in the fringe region of the 26-kilogauss magnetic field. These provide the hadronic trigger for the flash lamps of the bubble chamber, as well as trajectory data for charged secondary particles.

(iii) Cerenkov counters to identify π, K and p among the charged secondaries.

(iv) Lead glass detectors including active converter, position monitor,

and absorber, to provide photon detection and electron identification.

The entire system was brought into operation in the beam in May 1980. After initial check out of the apparatus, the first phase of data taking was begun on June 20, with 20CGeV photons and with high resolution optics (HRO). Approximately 100,000 pictures were taken before this run ended on July 16.

Several members of our group worked on the data taking run, including a graduate research assistant, Steve Kovner, David Brick and Anatole Shapiro. Our technician, David Rossi, spent some weeks at SLAC before the run, assisting on electronics and testing. Dave Brick is working on an off-line program for general use, to link the electronic track information with the bubble chamber information.

A rapid scan of some of the first film was carried out at SLAC to try to identify charm candidates. The results of this scan, on approximately 48,000 frames, are as follows:

1) 4700 events on HRO of which about 10% are obscured.
2) 256 events have a single V^o
3) 159 events have a single charged decay, $V^{\pm}$
4) 17 events have $V^o + V^o$
5) 24 events have $V^{\pm} + V^o$
6) 3 events have $V^{\pm} + V^{\pm}$
7) 1 event has $V^o + V^o$ + possible V^+.
8) 62 V^o decays are within 10 cm of the primary vertex on the HRO scan tables.
9) 85 $V^{\pm}$ decays are within 10 cm of the primary vertex.

So far no charm events have been definitely identified.

We have now received some film, both 35mm film with the single HRO view which we can easily scan on our standard equipment and 70 mm film containing the other three views on a single strip. We have modified one of our scan-measure tables to work with the 70 mm film, and have begun scanning. We will IPD this film for precision measurement at the MIT PEPR.

Since the initial run, work has been proceeding on various improvements in the beam and equipment. The system is to be checked out during the period October 1 - October 15, and the second-data taking run is then to begin about mid-October. The first few weeks of this run will be done at E_γ = 10.5 GeV, to look for a possible threshold enhancement effect,[1,2] provided the accelerator can deliver 23.5 GeV electrons unsledded. Starting about November 10, data taking at E_γ = 20 GeV is to begin.

More detailed discussion of the SLAC experiments is given in the accompanying Proposal.

REFERENCES

1. B. Ranek and M. Rabin, BC 72 Note 86, BC 73 Note 10, April 29, 1980.

2. H. Rubinstein and L. Stodolsky, Phys. Letters 76B, 479 (1978).

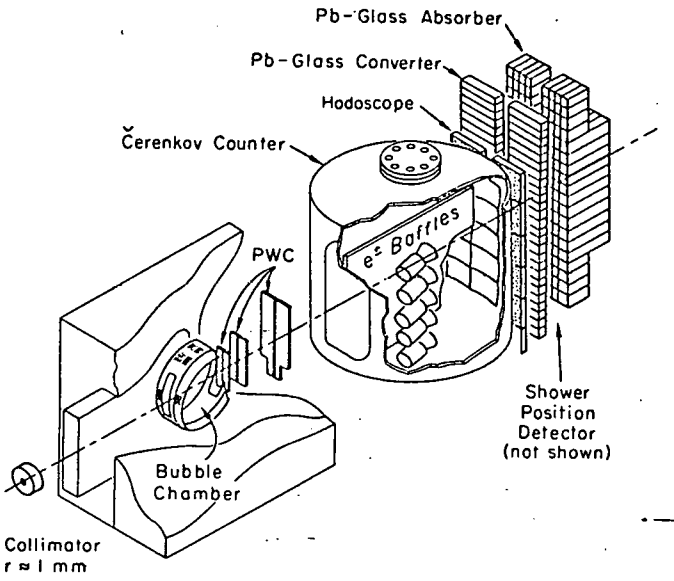
Pb-Glass Absorber
Pb-Glass Converter
Hodoscope
Čerenkov Counter
e± Baffles
PWC
Shower
Position
Detector
(not shown)
Bubble
Chamber
Collimator
r ≈ 1 mm

Fig. 1 (IIc)

(d) The Influence of Parton Structure on Hadronic Interactions in the European Hybrid Spectrometer (EHS) with a $K^+/\pi^+/p$ Beam at 250 GeV/c (CERN Proposal SPSC/80-51/P144).

We have joined our colleagues at MIT and with several groups in Europe and Israel in proposing this experiment to be carried out at CERN. The present proposal has as its principal aims a study of:

(a) the influence of parton structure on low p_T hadron-hadron collisions;

(b) quark-fragmentation functions from hadron-nucleus collisions;

(c) the production and decay of charm particles, including F mesons.

This experiment is to be done using the European Hybrid Spectrometer (EHS), which is a very powerful version of the Fermilab hybrid spectrometer system. The EHS combines large geometrical acceptance with good particle identification over a wide range of particle momentum, and high momentum resolution.

The components of the system, shown in Fig. 1, include a rapid cycling bubble chamber (RCBC), proportional and drift chambers (W1, W2, D1-D6) and spectrometer magnets (M1, M2). The bubble chamber, which has a cycling rate of >15 Hz, combines very good spatial resolution with a 4π acceptance. The trajectories of the forward going particles will be well determined in the two downstream lever arms; the error in the momentum measurement never exceeds 2%.

Good particle identification over the full momentum range is one of the most important features of the EHS. It is provided by RCBC for the lowest energy, combined with a silico-aerogel detector (SAD), a pictorial drift chamber (ISIS2), a forward Cerenkov (FC) and a transition radiation detector (TRD). The efficiency as a function of the momentum is given in Fig. 2 and Table I for the different detectors. In particular there is good

kaon identification over the complete momentum range.

The intermediate and forward gamma detectors IGD and FGD have good resolution and large geometrical acceptance in the central and forward regions. The π^o detection efficiency is typically 60%. Of particular importance are the following features:

- Energy measurement of the total π^o component is possible in the forward hemisphere.
- In case of one or two forward π^o's, kinematical reconstruction of π^o's is possible with the same precision as for charged tracks.
- Channels with no neutral pions can be cleaned up by π^o antiselection.

For the study of hadron-nucleus interactions, thin metal foils will be placed in the rapid cycling bubble chamber, in a manner similar to that planned for our Fermilab experiment, E-565.

High resolution optics are planned for the experiment also.

A beam of positive particles, with the K^+ component enriched to 15% is proposed. Tuning of the system on the beam without foils in the bubble chamber, and without the forward Cerenkov counter and transition radiation detector, is proposed for early 1981. A 30-day exposure is requested to follow this, with 1/3 to be taken as soon as the FC and TRD are ready (second half of 1981). The remaining 2/3 could be taken with two additional calorimeters (to be proposed) in the second half of 1982. This 30-day exposure will give a total of about 600K K^+ and π^+ induced events.

For the charm search, it is proposed to replace the RCBC with a new high resolution vertex detector, either a super LEBC or a small bubble chamber to be used with holographic techniques. This is still in an early design and

planning stage. An additional, later 30-day exposure is proposed with this detector used in conjunction with the spectrometer system.

A brief discussion of the physics of the experiment is given in the accompanying Renewal Proposal.

Table I: Momentum Range (in GeV/c) Of Particle Identification by Various Detectors.

Detector	π/Kp	$K/\pi p$	$p/\pi K$
FC	24 - 88	-	88 - 160
TRD	> 88	-	-
FC+TRD	> 24	88 - 160	88 - 160
All	all	0 - 160	0 - 160

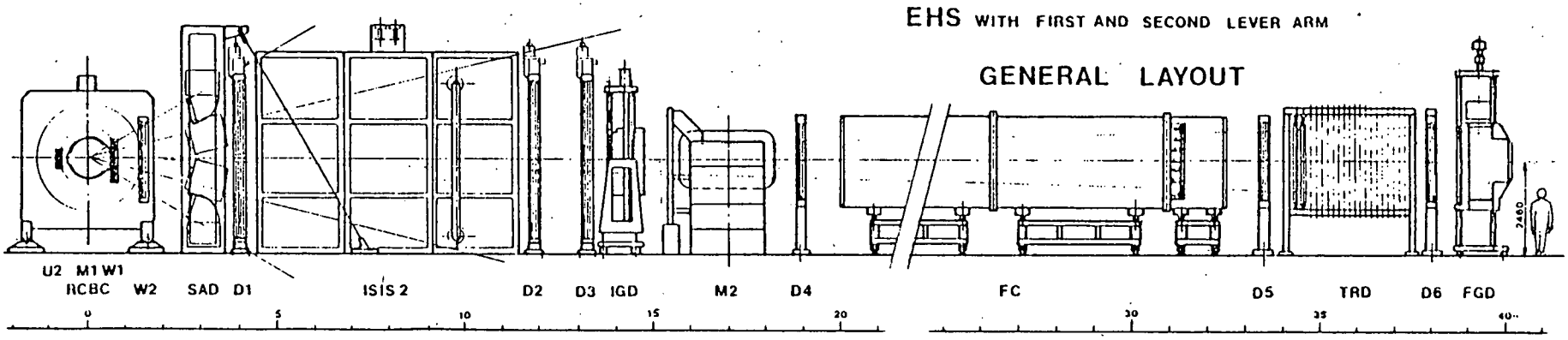
EHS WITH FIRST AND SECOND LEVER ARM
GENERAL LAYOUT
U2 M1 W1
RCBC W2 SAD D1 ISIS 2 D2 D3 IGD M2 D4 FC D5 TRD D6 FGD
0
5
10
15
20
30
35
40
2460

Fig. 1 (P II)

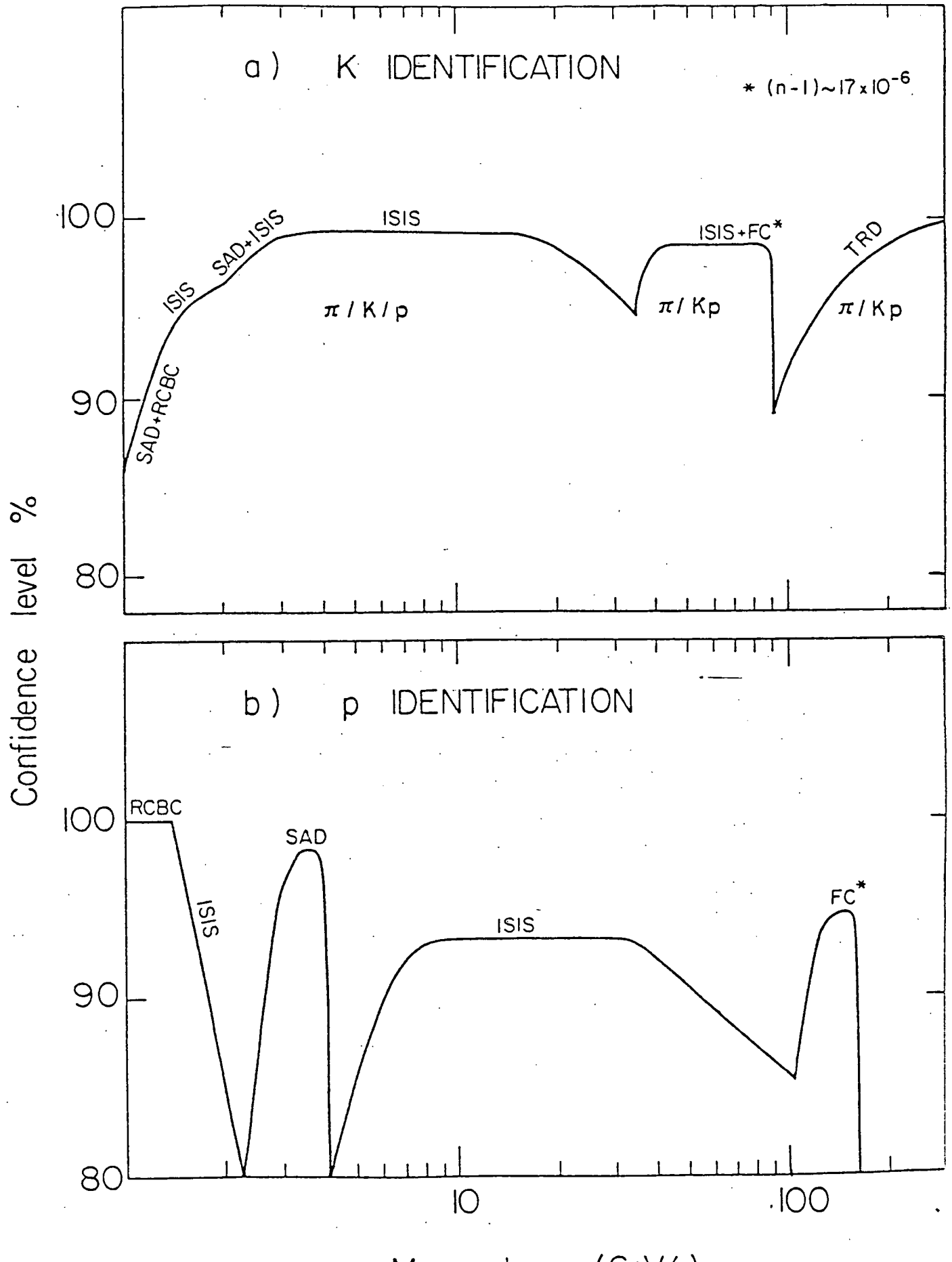
a) K IDENTIFICATION
* (n-1)~17x10^-6
100
90
80
SAD+RCBC
ISIS
SAD+ISIS
ISIS
π / K / p
ISIS+FC*
π / Kp
TRD
π / Kp
b) p IDENTIFICATION
RCBC
SISI
SAD
ISIS
FC*
100
90
80
10
100
Confidence level %
Momentum , (GeV/c)

Fig. 2 (II d)

III. Associated Matters.

During the past year almost all members of our group, including our technicians - Donovan Lewis and David Rossi, have spent considerable periods of time at Fermilab and SLAC working on our experiments in progress and in preparation. Dave Rossi has spent three weeks at SLAC and two weeks at FNAL preparing electronics and cables for the experiments; Donovan Lewis worked six weeks at Fermilab on similar projects. Steve Kovner, Dave Brick, and Anatole Shapiro worked a total of two months at SLAC making the initial run of BC 72 and 73 this spring and summer. Similar amounts of time will be spent by the group this fall and winter on the runs at the two national laboratories (Mildred Widgoff will be working at SLAC, FNAL, and CERN for several months next spring when she begins a sabbatical leave in January.)

Dave Brick spent considerable additional time at SLAC - over a month during several trips - working on data-reduction programs for the BC 72 and 73 experiments. He has contributed greatly to the research program over the past few years, and we have consequently recommended that he be promoted to Assistant Professor of Physics (Research). This appointment has been approved by the Physics Department and is now being processed by the University.

Several members of the group participated in various workshops at Fermilab in preparation for the submission of proposals for new experiments to be performed at the Fermilab Tevatron. Anatole Shapiro also attended the International Conference on Meson Spectroscopy, held at Brookhaven National Laboratory this April; while Dave Brick and Mildred Widgoff attended the XX International Conference on High Energy Physics, held at Madison, Wisconsin this July.

IV. Scientific Personnel Associated with the Bubble Chamber - Hybrid System Program.

A. M. Shapiro	- -	Professor
M. Widgoff	- -	Professor
H. S. Rudnicka	- -	Assistant Professor
D. H. Brick	- -	Research Associate
D. Lewis	- -	Research Assistant
S. Kovner	- -	Graduate Research Assistant
M. Heller	- -	Graduate Student

V. Papers Published During the Preceding Year and Papers in Press.

320.* D. Brick, D. Fong, M. Heller, A. M. Shapiro, M. Widgoff, and coauthors, "Neutral-Particle Production in $\pi^- p$ Interactions at 147 GeV/c and Comparison to Charged-Particle Production," Phys. Rev. D20, 2123 (1979).

321.* D. Brick, A. M. Shapiro, M. Widgoff, and coauthors, "Inclusive Production of Neutral Strange Particles by 147 GeV/c $\pi^+/K^+/p$ Interactions in Hydrogen," Nucl. Phys. B164, 1 (1980).

322.* D. Brick, A. M. Shapiro, M. Widgoff, and coauthors, "Inclusive Δ^{++} Production in pp, $K^+ p$, $\pi^+ p$, and $\pi^- p$ Interactions at 147 GeV/c," Phys. Rev. D21, 632 (1980).

324. D. Brick, D. Fong, M. Heller, A. M. Shapiro, M. Widgoff, and coauthors, "Leading Particles and Diffraction Dissociation in 150-GeV/c $\pi^- p$ Interactions," Phys. Rev. D21, 1726 (1980).

325. M. Heller, "A Prism Plot Analysis of the Reaction $\pi^+ p \to p\pi^+\pi^o$ at 4.1 GeV/c," Experimental High Energy Physics Group Internal Report #B-1 (Ph.D. Dissertation, Brown University, June 1980) (unpublished).

326. A. M. Shapiro and coauthors, "Cross Sections for $\pi^- + p \to n + k\pi^o$ (k = 1 to 5) and $\pi^- + p \to n + \eta^o$ ($\eta^o \to 2\gamma$) for Incident Pion Momenta between 1.3 and 3.8 GeV/c," Phys. Rev. D21, 3023 (1980).

327. A. M. Shapiro, M. Widgoff, and coauthors, "High Transverse Momentum Jets in 147 GeV/c Interactions," Bull. Am. Phys. Soc. 25, 33 (1980).

328. D. Brick, M. Widgoff, and coauthors, "Extraction of Off-Mass-Shell $\pi\pi$ and $K\pi$ Interactions, "Bull. Am. Phys. Soc. 25, 33 (1980).

329. D. Brick, A. M. Shapiro, and coauthors, "Study of Resonances Produced in Four-Prong $\pi^\pm p$, $K^\pm p$, and pp Interactions at 147 GeV/c," Bull. Am. Phys. Soc. 25, 33 (1980).

330. D. Brick, M. Widgoff, and coauthors, "Inclusive ρ^o Production in $\pi^\pm p$, $K^\pm p$, and pp Interactions at 147 GeV/c," Bull. Am. Phys. Soc. 25, 34 (1980).

331. D. Brick, A. M. Shapiro, and coauthors, "Inclusive Strange Resonance Production in 147 GeV/c $\pi^\pm p$, $K^\pm p$, and pp Interactions," Bull. Am. Phys. Soc. 25, 561 (1980).

332. M. Widgoff, H. Rudnicka, and coauthors, "Average Inclusive Charged-Particle Multiplicities in $\pi^\pm p$, $K^\pm p$, and pp Interactions at 147 GeV/c," Bull. Am. Phys. Soc. 25, 561 (1980).

333. M. Widgoff and coauthors, "Inclusive π^+/π^- Ratios in 147 GeV/c $\pi^\pm p$, $K^\pm p$, and pp Interactions," Bull. Am. Phys. Soc. 25, 580 (1980).

334. A. M. Shapiro and coauthors, "Exclusive Final States in $\pi^+ p$, $K^+ p$, and pp Interactions at 147 GeV/c," Bull. Am. Phys. Soc. 25, 580 (1980).

335. D. Brick, A. M. Shapiro, M. Widgoff, and coauthors, "Hadron Production in $\pi^\pm p$, $K^\pm p$, and pp Collisions at 147 GeV/c and Properties of Jet-like Multiparticle Systems," XX International Conference on High Energy Physics, Madison, Wisconsin, July 1980 (to be published).

336. D. Brick, A. M. Shapiro, M. Widgoff, and coauthors, "Inclusive and Semi-Inclusive ρ^o Production in $K^\pm/\pi^\pm/p$ Interactions at 147 GeV/c," Z. Physik C (in press).

337. D. Brick, A. M. Shapiro, M. Widgoff, and coauthors, "Approach to Scaling in Inclusive π^+/π^- Ratios," Z. Physik C (in press).

338. D. Brick, H. Rudnicka, A. N. Shapiro, M. Widgoff, and coauthors, "Double Pomeron Exchange in the Reactions $pp \to pp\pi^+\pi^-$, $K^+ p \to K^+ p\pi^+\pi^-$, $\pi^+ p \to \pi^+ p\pi^+\pi^-$, and $\pi^- p \to \pi^- p\pi^+\pi^-$ at 147 GeV/c," Phys. Rev. Lett. (in press).

339. D. Brick, A. M. Shapiro, M. Widgoff, and coauthors, "Multiple Correlations and High Transverse Momentum Jets in 147 GeV/c $\pi^- p$ Interactions," Phys. Rev. D (final draft - to be submitted).

340. A. M. Shapiro and M. Widgoff, "Progress Report of a Research Program in Experimental High Energy Physics," October 1980.

* These three papers were listed in last year's Progress Report, under these numbers, as being in press.